CrossMark

Ginsenoside Re protects methamphetamine-induced dopaminergic neurotoxicity in mice via upregulation of dynorphin-mediated κ-opioid receptor and downregulation of substance P-mediated neurokinin 1 receptor

Duy-Khanh Dang[1†], Eun-Joo Shin[1†], Dae-Joong Kim[2], Hai-Quyen Tran[1], Ji Hoon Jeong[3], Choon-Gon Jang[4], Seung-Yeol Nah[5], Jung Hwan Jeong[6], Jae Kyung Byun[7], Sung Kwon Ko[8*], Guoying Bing[9], Jau-Shyong Hong[10] and Hyoung-Chun Kim[1*] (iD)

Abstract

Background: We previously reported that ginsenoside Re (GRe) attenuated against methamphetamine (MA)-induced neurotoxicity via anti-inflammatory and antioxidant potentials. We also demonstrated that dynorphin possesses anti-inflammatory and antioxidant potentials against dopaminergic loss, and that balance between dynorphin and substance P is important for dopaminergic neuroprotection. Thus, we examined whether GRe positively affects interactive modulation between dynorphin and substance P against MA neurotoxicity in mice.

Methods: We examined changes in dynorphin peptide level, prodynorphin mRNA, and substance P mRNA, substance P-immunoreactivity, homeostasis in enzymatic antioxidant system, oxidative parameter, microglial activation, and pro-apoptotic parameter after a neurotoxic dose of MA to clarify the effects of GRe, prodynorphin knockout, pharmacological inhibition of κ-opioid receptor (i.e., nor-binaltorphimine), or neurokinin 1 (NK1) receptor (i.e., L-733,060) against MA insult in mice.

(Continued on next page)

* Correspondence: skko@semyung.ac.kr; kimhc@kangwon.ac.kr
†Equal contributors
8Department of Oriental Medical Food and Nutrition, Semyung University, Jecheon 27136, Republic of Korea
1Neuropsychopharmacology and Toxicology Program, College of Pharmacy, Kangwon National University, Chunchon 24341, Republic of Korea
Full list of author information is available at the end of the article

Dang *et al. Journal of Neuroinflammation* (2018) 15:52

Page 2 of 22

(Continued from previous page)

Results: GRe attenuated MA-induced decreases in dynorphin level, prodynorphin mRNA expression in the striatum of wild-type (WT) mice. Prodynorphin knockout potentiated MA-induced dopaminergic toxicity in mice. The imbalance of enzymatic antioxidant system, oxidative burdens, microgliosis, and pro-apoptotic changes led to the dopaminergic neurotoxicity. Neuroprotective effects of GRe were more pronounced in prodynorphin knockout than in WT mice. Nor-binaltorphimine, a κ-opioid receptor antagonist, counteracted against protective effects of GRe. In addition, we found that GRe significantly attenuated MA-induced increases in substance P-immunoreactivity and substance P mRNA expression in the substantia nigra. These increases were more evident in prodynorphin knockout than in WT mice. Although, we observed that substance P-immunoreactivity was co-localized in NeuN-immunreactive neurons, GFAP-immunoreactive astrocytes, and Iba-1-immunoreactive microglia. NK1 receptor antagonist L-733,060 or GRe selectively inhibited microgliosis induced by MA. Furthermore, L-733,060 did not show any additive effects against GRe-mediated protective activity (i.e., antioxidant, antimicroglial, and antiapoptotic effects), indicating that NK1 receptor is one of the molecular targets of GRe.

Conclusions: Our results suggest that GRe protects MA-induced dopaminergic neurotoxicity via upregulatgion of dynorphin-mediated κ-opioid receptor and downregulation of substance P-mediated NK1 R.

Keywords: Methamphetamine, Dynorphin, κ-opioid receptor, Microglia, Neurokinin 1 receptor

Background

Dynorphin is an endogenous opioid peptide that is widely distributed in various tissues. Numerous studies have suggested the involvement of dynorphin in the pathogenesis of Parkinson's disease (PD). Earlier studies reported that reduced mRNA levels of prodynorphin were observed in the substantia nigra (SN) in postmortem brain specimens of Parkinsonian patients and animal models of PD [1, 2]. We reported that endogenous dynorphin attenuates dopaminergic neurotoxicity induced by 1-methyl-4-phenyl-1, 2, 3, 6-tetrahydropyridine (MPTP) or methamphetamine (MA) [3], and that genetic depletion of dynorphin potentiated induction of pro-inflammatory microglia of M1 phenotype (CD16, CD32, and CD86) [3].

Substance P is a potent pro-inflammatory neuropeptide with high concentrations in the SN [4, 5]. Previous reports have demonstrated that substance P receptor (neurokinin-1 receptor) antagonists prevented MA-induced loss of neurochemical markers of toxicity such as tyrosine hydroxylase, dopamine transporters, and tissue dopamine content in the striatum [6, 7]. Hong and colleagues [8–14] demonstrated the pathogenic role of microglia-induced neuroinflammation in multiple neurodegenerative disorders, including PD. Substance P is capable of stimulating microglial activation to produce superoxide and pro-inflammatory cytokines, thereby exacerbating dopaminergic neurodegeneration [13, 14]. We recently demonstrated that substance P might account for the increased density of microglia in the SN through chemotaxic recruitment via a novel NK1-NOX2 axis-mediated pathway [15].

Evidence has been reported which suggests the existence of a dopaminergic influence on the substance P striatonigral neurons [4, 16–19]. After chronic administration of the antipsychotic haloperidol, a potent dopamine receptor antagonist, nigral substance P-like immunoreactivity (SP-IR) was reduced substantially [20–22]. The enhancement of dopamine activity with repeated administrations of the indirect dopamine agonist methamphetamine (MA) causes elevations of SP-IR in several structures associated with the basal ganglia including SN [16]. This MA effect was blocked by concurrent administration of haloperidol, suggesting that the action of the drug on the striatonigral substance P neurons is mediated through the dopamine system [16]. Importantly, Block et al. [23] found that dynorphin inhibited substance P-induced dopaminergic neurotoxicity in vivo, suggesting the balance between dynorphin and substance P is essential for dopaminergic regulation.

Ginsenoside Re (GRe), a potential ginsenoside from Panax ginseng, exhibited different pharmacological activities via multiple mechanisms both in vivo and in vitro [24–29]. We reported that GRe rescues MA-induced dopaminergic degeneration and pro-inflammatory changes (i.e., activation of microglia) in vivo by inhibition of protein kinase Cδ [30]. Interestingly, our pilot study showed that GRe attenuated MA-induced decrease in prodynorphin mRNA expression in the striatum of wild-type mice [31].

To extend our knowledge, we investigated whether GRe requires dynorphin induction for protecting MA-induced dopaminergic toxicity. In addition, we also asked whether GRe modulates interaction between dynorphin/κ-opioid receptor and substance P/neurokinin 1 (NK1) receptor against MA toxicity. Here, we proposed that GRe-mediated neuroprotective effects in vivo against MA-induced dopaminergic toxicity require

Dang *et al. Journal of Neuroinflammation* (2018) 15:52

Page 3 of 22

interactive modulation between dynorphin and substance P via upregulation of κ-opioid receptor and downregulation of NK1 receptor.

Methods
Animals
All animals were treated in accordance with the National Institutes of Health (NIH) Guide for the Humane Care and Use of Laboratory Animals (NIH Publication No. 85-23, 1985; grants.nih.gov/grants/olaw/references/PHSPolicyLabAnimals.pdf). The present study was performed in accordance with the Institute for Laboratory Research (ILAR) Guidelines for the Care and Use of Laboratory Animals. Mice were maintained under a 12-h light/12-h dark cycle and fed ad libitum. They were adapted to these conditions for 2 weeks prior to the experiment.

The prodynorphin knockout (DYN KO) mice were originally obtained by targeted deletion of the coding exons of the prodynorphin gene [32]. We used this animal model in our previous studies [33, 34]. The DYN KO strain used in the present study was backcrossed at least nine times to the C57BL/6 background. Prior to weaning, tail specimens were collected from each animal, and DNA was extracted to confirm the presence of the prodynorphin gene locus by polymerase chain reaction (PCR) using primer pairs specific for each genotype [32–34]. Primers to detect WT alleles at the prodynorphin gene locus were 5′-CAGGACCTGGT GCCGCCCTCAGAG-3′ and 5′-CGCTTCTGGTTGTCC CACTTCAGC-3′; primers specific for the deletion were 5′-ATCCAGGAAACCAGCAGCGGCTAT-3′ and 5′-ATT CAGACACATCCCACATAAGGACA-3′. The products were amplified in a GeneAmp PCR System 9700 (Applied Biosystems, Foster City, CA, USA) using the following PCR parameters: an initial denaturation at 94 °C for 5 min, and then 30 cycles of 94 °C for 30 s, 65 °C for 30 s, 72 °C for 30 s, and 72 °C for 5 min followed by electrophoresis on 1% agarose gels with ethidium bromide and photography under ultraviolet (UV) light.

Drug treatment
Mice were treated with a single dose of MA (35 mg/kg, i.p.) or saline, and sacrificed 1 h, 3 h, 6 h, 12 h, 1 day, and 3 days after MA treatment to examine prodynorphin and substance P mRNA expressions, ROS formation, and HNE and protein carbonyl levels. High-performance liquid chromatography grade GRe with greater than 99% purity was provided by Dr. Sung Kwon Ko [35, 36]. GRe (20 mg/kg, i.p., twice a day) was given 5 days before and 1 day after MA injection. On the day of MA injection, GRe was administered at 2 h before and 10 h after MA injection. The dose of GRe was determined based on previous study [30]. Nor-binaltorphimine (Nor-B; κ-opioid

receptor antagonist; Tocris Bioscience, Ellisville, MO, USA) was dissolved in sterile saline. Nor-B (3 or 6 mg/kg, i.p.) was given 3 h and 1.5 h before MA injection. The dose of Nor-B was determined based on previous study [34]. L-733,060 (NK1 receptor antagonist; Tocris Bioscience) was dissolved in sterile saline. L-733,060 (5 or 10 mg/kg, i.p.) was given 1 h before MA injection. The dose of L-733,060 was determined based on previous study [37].

Dynorphin quantification
For sample preparation, brains were removed and placed into ice-cold oxygenated artificial cerebrospinal fluid (aCSF) for approximately 1 min before slicing. The dorsal striatum, NAc, and ventral midbrain were free-hand dissected from 400-μm-thick slices of brain tissue prepared using a vibrating tissue slicer. Tissue samples were placed in individual eppendorf tubes, flash-frozen in liquid nitrogen, and stored at – 80 °C until further use. All tissues were homogenized in RIPA buffer [150 mM NaCl, 1.0% Triton-X-100, 0.5% Sodium Deoxycholate, 0.1% Sodium Dodecyl Sulfate (SDS), 50 mM Trizma Base, pH 8.0] and centrifuged at 12,000×*g* for 30 min. The pellet was discarded and supernatant used in the enzyme-linked immunosorbant assay (ELISA). Protein was measured using the BCA protein assay reagent (Thermo Scientific, Rockford, IL, USA).

For enzyme-linked immunosorbant assay, a commercially available mouse-dynorphin ELISA kit (MBS727820; MyBioSource, Inc., San Diego, CA, USA) was utilized to determine the concentration of dynorphin in the tissue samples from WT mice. Briefly, standards and samples (5 μg protein/sample) were pipetted in duplicate into the 96-well plate provided. All reagents were added to wells, and the plate was washed and incubated according to kit instructions. The optical density of the samples was read within 4 min of the final incubation at 450 nm using a microplate reader (Molecular Devices Inc., Sunnyvale, CA, USA) [38].

Tissue preparation for enzyme activity assays
Dorsal striatum, nucleus accumbens (NAc), and ventral midbrain were homogenized in 50 mM potassium phosphate buffer (pH 7.0) and centrifuged at 13,000 × *g* for 20 min. The resulting supernatant was used to measure the activities of glutathione peroxidase (GPx) and catalase. Additional dorsal striatum, NAc, and ventral midbrain were homogenized in 50 mM potassium phosphate buffer (pH 7.8) and were centrifuged at 13,000 × *g* for 20 min. The resulting supernatant was used to measure the activities of superoxide dismutase (SOD) [30].

Dang *et al. Journal of Neuroinflammation* (2018) 15:52

Page 4 of 22

Determination of SOD activity

SOD activity was determined on the basis of inhibition of superoxide-dependent reactions as described previously [30] The reaction mixture contained 70 mM potassium phosphate buffer (pH 7.8), 30 μM cytochrome c, 150 μM xanthine, and tissue extract in phosphate buffer diluted tenfold with PBS in a final volume of 3 mL. The reaction was initiated by adding 10 μL of 50 units xanthine oxidase, and the change in absorbance at 550 nm was recorded. One unit of SOD was defined as the quantity required inhibiting the rate of cytochrome c reduction by 50%. For estimating total SOD, 10 μM potassium cyanide (KCN) was added to the medium to inhibit cytochrome oxidase activity.

Determination of catalase activity

Catalase activity was determined by the rate of hydrogen peroxide absorbance decrease at 240 nm [30]. The reaction mixture contained 50 mM potassium phosphate buffer (pH 7.0) and an aliquot of the sample. The reaction started with adding hydrogen peroxide (final concentration of 10 mM), and absorbance was monitored at 25 °C for 5 min. Catalase from bovine liver (Sigma-Aldrich, St. Louis, MO, USA) was used as a standard.

Determination of glutathione peroxidase (GPx) activity

GPx activity was analyzed by a spectrophotometric assay described by Shin et al. [30], using 2.0 mM reduced glutathione and 0.25 mM cumene hydroperoxide as substrates. The reaction rate at 340 nm was determined using the NADPH extinction coefficient (6.22 mM^{-1} cm^{-1}). GPx activity was expressed as nanomole NADPH oxidized per minute per milligram protein at 25 °C. Protein was measured using the BCA protein assay reagent, and bovine serum albumin was used as a standard.

Western blot analysis

Striatal tissues were lysed in buffer containing a 200 mM Tris–HCl (pH 6.8), 1% SDS, 5 mM ethylene glycol-bis (2-aminoethyl ether)-N, N, N′, N′-tetraacetic acid (EGTA), 5 mM EDTA, 10% glycerol, 1 × phosphatase inhibitor cocktail I (Sigma-Aldrich, St. Louis, MO, USA), and 1 × protease inhibitor cocktail (Sigma-Aldrich). Lysate was centrifuged at 12,000×g for 30 min, and the supernatant fraction was utilized for western blot analysis as described previously [30, 39]. Proteins (20 μg/ lane) were separated by 8 or 10% SDS-PAGE, and transferred onto PVDF membranes. Following transfer, the membranes were preincubated with 5% non-fat milk for 30 min and were incubated overnight at 4 °C with primary antibody against NeuN (1:200; EMD Millipore, Temecular, MA, USA), GFAP (1:500; Santa Cruz Biotechnology, Santa Cruz, CA, USA), Iba-1 (1:500; Abcam, Cambridge, MA, USA), Bax (1:1000; Santa Cruz

Biotechnology), cleaved caspase-3 (1:1000; Cell Signaling Technology, Inc., Danvers, MA, USA), caspase-3 (1:1000; Cell Signaling Technology, Inc.), Bcl-2 (1:1000; Santa Cruz Biotechnology), TH [5000; Chemicon (EMD Millipore)], or β-actin (1:50000; Sigma-Aldrich). Membranes were then incubated with HRP-conjugated secondary anti-rabbit IgG (1:1000, GE Healthcare, Piscataway, NJ, USA), anti-mouse IgG (1:1000, Sigma-Aldrich), or anti-goat IgG (1:1000, Sigma-Aldrich) for 2 h. Subsequent visualization was conducted using an enhanced chemiluminescence system (ECL plus®, GE Healthcare, Arlington Heights, IL, USA). Relative intensities of the bands were quantified by Photo-Capt MW (version 10.01 for Windows; Vilber Lourmat, Marne la Vallée, France) and then normalized to the intensity of β-actin [30].

Immunocytochemistry

Immunocytochemistry was performed as described previously [30]. Mice were perfused transcardially with 50 mL of ice-cold PBS (10 mL/10 g body weight) followed by 4% paraformaldehyde (20 mL/10 g body weight). Brains were removed and stored in 4% paraformaldehyde overnight. A series of every sixth section (35 μm thickness, 210 μm apart) from striatum was selected and subjected to immunocytochemistry. Sections were blocked with PBS containing 0.3% hydrogen peroxide for 30 min and then incubated in PBS containing 0.4% Triton X-100 and 1% normal serum for 20 min. After a 48-h incubation with primary antibody against TH [1:500; Chemicon (EMD Millipore)], Iba-1 (1:500, Wako Pure Chemical Industries, Chuo-ku, Osaka, Japan), or substance P (1:500, a kind gift from Dr. Jau-Shyong Hong, National Institute of Environmental Health Sciences, USA; this antibody has been described elsewhere [15]). Sections were incubated with the biotinylated secondary antibody (1:1000; Vector Laboratories, Burlingame, CA, USA) for 1 h. The sections were then immersed in a solution containing avidin–biotin peroxidase complex (Vector Laboratories) for 1 h, and 3,3′-diaminobenzidine was utilized as the chromogen. Digital images were acquired under an upright microscope (BX51; Olympus, Tokyo, Japan) using an attached digital microscope camera (DP72; Olympus) and an IBM-compatible PC.

ImageJ software, version 1.47 (National Institutes of Health, Bethesda, MD, USA) was employed to measure the immunoreactivities of TH and Iba-1 in the striatum, or substance P in the SN as described previously [3, 15, 40, 41]. Briefly, images were subjected to background subtraction to correct for uneven background. The entire striatal region (for TH-immunoreactivity) or the rectangular region (350 μm × 260 μm, $w × h$, for Iba-1-or substance P-immunoreactivity) was drawn as the region of interest (ROI). Hue, saturation, and brightness

Dang *et al. Journal of Neuroinflammation* (2018) 15:52

Page 5 of 22

threshold values were set in the "Adjust Color Threshold" dialog box to select the immunoreactive area, and then the mean density was measured.

Double-labeled immunocytochemistry

Brain sections of 5 μm thickness obtained from wild-type (B6) mice were placed on the same slide and processed for immunostaining. Tissues were adhered on poly-L-lysine-precoated coverslips, were fixed in PBS-4% para-formaldehyde (PFA), and were permeabilized with 0.1% Triton X-100 in PBS for 15 min. After saturation with PBS-1% BSA, tissues were incubated for 40 min with the primary antibody and were incubated for 40 min with the secondary antibody as follows: primary antisera were as follows: rabbit anti-substance P ([15]; diluted 1:100), mouse anti-NeuN (1:100, Chemicon), goat anti-GFAP (1:100, Abcam), and mouse anti-Iba1 (1:100, Abcam). Secondary antibodies were goat anti-mouse IgG H&L (Alexa Fluor® 568; 1:100, Invitrogen, Carlsbad, CA, USA), goat anti-rabbit IgG H&L (FITC; 1:500, Abcam), and donkey anti-goat IgG H&L (Alexa Fluor® 546; 1:200, Invitrogen). Images of samples were recorded using an FV1000 confocal microscope (Olympus). To minimize bleed-through, each signal in double- or triple-stained samples was imaged sequentially. Images were processed in accordance with the Guidelines for Proper Digital Image Handling using ImageJ and/or Adobe Photoshop CS3 (Adobe, San Jose, CA, USA).

Dissection of substantia nigra (SN)

Brains were rapidly removed and cut into 1 mm coronal sections on ice. The SN was punched using a fine Pasteur pipette. The SN was then easily identified and freely dissected. The total time for isolation of the SN was less than 3 min. The tissues were stored at − 70 °C until analysis [42–44].

Reverse transcription and polymerase chain reaction (RT-PCR)

Expression of prodynorphin and substance P was assessed using quantitative RT–PCR to analyze mRNA levels, as described previously [45]. Total RNA was isolated from striatal or nigral tissues using an RNeasy Mini Kit (Qiagen, Valencia, CA, USA) according to the manufacturer's instructions. Reverse transcription reactions were carried out using the RNA to cDNA EcoDry Premix (Clontech, Palo Alto, CA, USA) with a 1-h incubation at 42 °C. PCR amplification was performed using 25 cycles of denaturation at 94 °C for 1 min, annealing at 60 °C for 2 min, and extension at 72 °C for 1 min. The primer sequences and predicted product sizes for the amplified genes were as follows: prodynorphin (510 bp), 5′-CAG GAC CTG GTG CCG CCC TCA

GAG-3′ (forward) and 5′-CGC TTC TGG TTG TCC CAC TTC AGC-3′ (reverse); substance P (194 bp), 5′-AAG CCT CAG CAG TTC TTT GGA T-3′ (forward) and 5′-GTT CTG CAT CGC GCT TCT TTC-3′ (reverse); and glyceraldehyde 3-phosphate dehydrogenase (GAPDH; 450 bp), 5′-ACC ACA GTC CAT GCC ATC-3′ (forward) and 5′-TCC ACC ACC CTG TTG CTG TA-3′ (reverse). PCR products were separated on 2% agarose gels containing ethidium bromide and visualized under ultraviolet light. Quantitative analysis of RNA was performed using PhotoCapt MW (version 10.01 for Windows; Vilber Lourmat).

Synaptosome preparation

Striatal tissue was homogenized in 10 volume of ice-cold 0.32 mol/L sucrose and centrifuged at low speed ($800 \times g$, 12 min, 4 °C). This resulted in supernatant (S1) that was removed and centrifuged at high speed ($22,000 \times g$, 20 min, 4 °C) in order to yield pelleted synaptosomes. An aliquot of the re-suspended (P2) synaptosomal fraction was used for determination of ROS formation [39].

Determination of ROS formation

ROS formation in the synaptosome was assessed by measuring the conversion from 2′,7′-dichlorofluorescin diacetate (DCFH-DA) to dichlorofluorescin (DCF) [46]. Synaptosomal fractions were added to a tube containing 2 mL of phosphate-buffered saline (PBS) with 10 nmol of DCFH-DA, dissolved in methanol. The mixture was incubated at 37 °C for 3 h, and then fluorescence was measured at 480 nm excitation and 525 nm emission. DCF was used as a standard.

Determination of 4-hydroxynonenal (HNE)

The amount of lipid peroxidation was determined by measuring the level of 4-hydroxynonenal (HNE) using the OxiSelect™ HNE adduct ELISA kit (Cell Biolabs, Inc., San Diego, CA, USA) according to the manufacturer's instructions. 100 μL of striatal homogenate at a protein concentration of 10 μg/mL was incubated in a 96-well protein binding plate at 4 °C overnight. After protein adsorption, HNE adducts in each well were labeled with HNE antibody followed by HRP-conjugated secondary antibody. Colorimetric development was then performed with substrate solution. Absorbance was recorded at 450 nm using a microplate reader (Molecular Devices Inc.), and an amount of HNE adduct in each sample was calculated from the standard curve of HNE-BSA [30].

Determination of protein carbonyl

The extent of protein oxidation was assessed by measuring the content of protein carbonyl groups, which was determined spectrophotometrically with the 2,4-dinitrophenylhydrazine (DNPH)-labeling procedure [30] as

Dang et al. Journal of Neuroinflammation (2018) 15:52

Page 6 of 22

described by Oliver [47]. The results are expressed as nmol of DNPH incorporated/mg protein based on the extinction coefficient for aliphatic hydrazones of 21 mM^{-1} cm^{-1}. Protein was measured using the BCA protein assay reagent (Thermo Scientific, Rockford, IL, USA).

Measurement of dopamine (DA) and its metabolites

Mice were sacrificed by cervical dislocation, and the brains were removed. The dorsal striatum, NAc, and ventral midbrain were dissected as above, were immediately frozen in liquid nitrogen, and were stored at − 70 °C before assays. Tissues were weighed, ultrasonicated in 10% perchloric acid, and centrifuged at 20,000×g for 10 min. The levels of DA and its metabolites DOPAC and HVA were determined by HPLC coupled with an electrochemical detector, as described previously [3, 30, 43]. Supernatant aliquots (20 μL) were injected into an HPLC equipped with a C18 column with 3 μm particle size (Waters). The mobile phase was comprised of 26 mL of acetonitrile, 21 mL of tetrahydrofuran, and 960 mL of 0.15 M monochloroacetic acid (pH 3.0) containing 50 mg/L of EDTA and 200 mg/mL of sodium octyl sulfate. The amount of DA was determined by comparison of peak areas of tissue samples with standard and was expressed in ng/g of wet tissue.

Statistical analyses

Data were analyzed using IBM SPSS ver. 21.0 (IBM, Chicago, IL, USA). One-way analysis of variance (ANOVA) or two-way ANOVA was employed for statistical analyses. Post-hoc Fisher's least significant difference (LSD) pairwise comparison tests were then conducted. p values < 0.05 were considered to be significant.

Results

MA-induced changes in dynorphin level, prodynorphin mRNA, and substance P mRNA expression in the dorsal striatum of wild-type (WT) mice

We demonstrated a protective role of dynorphin in the modulation of dopaminergic system [3]. As shown in Fig. 1, we conducted a time-course study to elucidate changes in dynorphin level prodynorphin mRNA and substance P mRNA. Dynorphin level was significantly decreased 3 h ($p < 0.05$), 6 h ($p < 0.01$), 12 h ($p < 0.05$), and 1 day ($p < 0.05$) after a toxic dose of MA (Fig. 1a). The most pronounced decrease in dynorphin level was noted 6 h post-MA. Importantly, MA-induced decrease in dynorphin level in the dorsal striatum was most evident among nucleus accumbens, ventral midbrain, and dorsal striatum (please refer to Additional file 1: Figure S1). Interestingly, MA treatment did not change prodynorphin mRNA expression 3 and 6 h later, indicating that

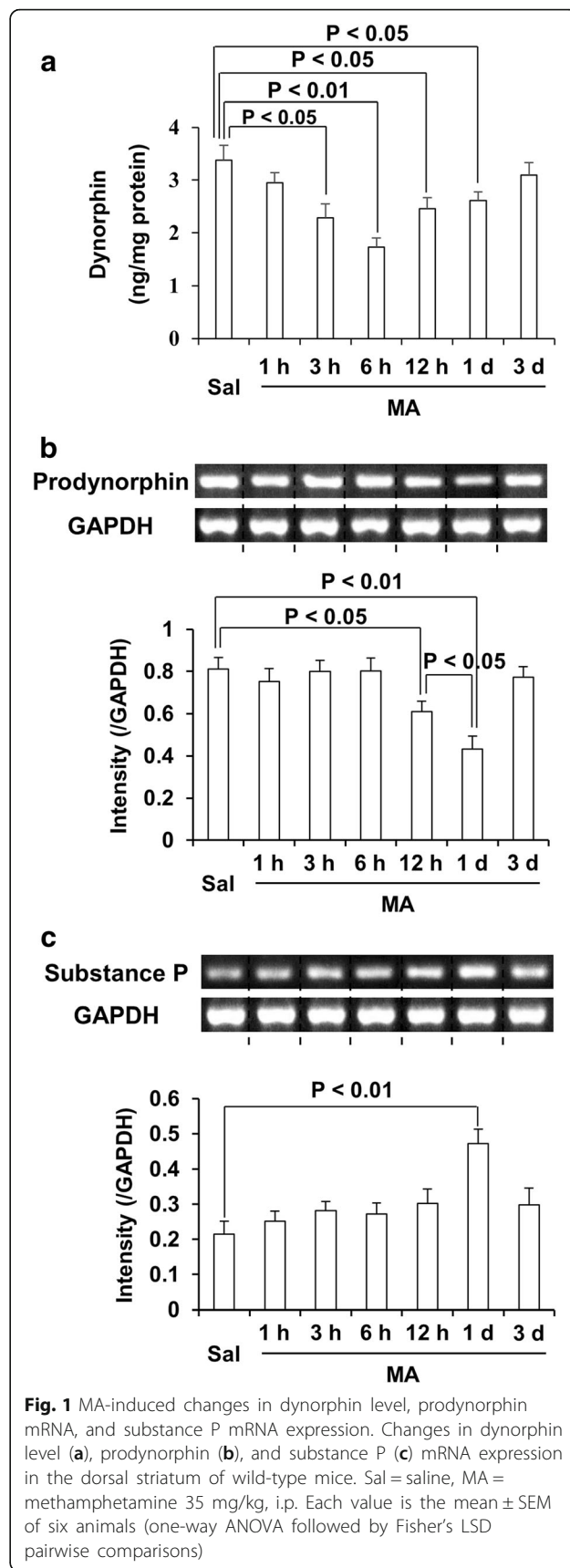**Fig. 1** MA-induced changes in dynorphin level, prodynorphin mRNA, and substance P mRNA expression. Changes in dynorphin level (**a**), prodynorphin (**b**), and substance P (**c**) mRNA expression in the dorsal striatum of wild-type mice. Sal = saline, MA = methamphetamine 35 mg/kg, i.p. Each value is the mean ± SEM of six animals (one-way ANOVA followed by Fisher's LSD pairwise comparisons)

Dang *et al. Journal of Neuroinflammation* (2018) 15:52

Page 7 of 22

compensatory induction to significant decreases in dynorphin level. MA-induced significant decreases in prodynorphin mRNA expression was observed 12 h ($p < 0.05$) and 1 day ($p < 0.01$) later (Fig. 1b). This decrease was more pronounced in 1 day post-MA ($p < 0.05$) than in 12 h post-MA (Fig. 1b). As presented in Fig. 1c, a significant increase ($p < 0.01$) in substance P mRNA expression was noted 1 day after MA of WT mice. Therefore, we have focused on 1 day time-point for further study.

Effects of genetic depletion of prodynorphin on MA-induced changes in superoxide dismutase (SOD), catalase, and glutathione peroxidase (GPx) activity in the dorsal striatum, nucleus accumbens (NAc), and ventral midbrain in mice

As shown in Table 1A–C, MA treatment initially increased ($p < 0.05$ vs. saline) SOD activity and decreased

GPx activity 3 h later in the dorsal striatum ($p < 0.05$ vs. saline), NAc ($p < 0.05$ vs. saline) and ventral midbrain ($p < 0.05$ vs. saline) of WT mice. MA treatment initially increased ($p < 0.05$) catalase activity 6 h later in the ventral midbrain, however, initially increased catalase activity 3 h later in the dorsal striatum ($p < 0.05$ vs. saline) and NAc ($p < 0.05$ vs. saline) of WT mice. All of these changes returned near saline level 3 days later. These changes appeared to be more pronounced in dorsal striatum than in NAc or ventral midbrain.

In addition, MA treatment exhibited in a sustained increases in SOD activity 6 h (dorsal striatum, NAc, or ventral midbrain; $p < 0.01$ vs. corresponding saline), 12 h (dorsal striatum or ventral midbrain; $p < 0.01$ vs. corresponding saline. NAc; $p < 0.05$ vs. corresponding saline), and 1 day (dorsal striatum or ventral midbrain; $p < 0.01$ vs. corresponding saline. NAc; $p < 0.05$ vs. corresponding

Table 1 Effect of genetic depletion of prodynorphin on MA-induced changes in activity in enzymatic antioxidants

			A					
SOD (units/mg protein)		Saline	MA					
			1 h	3 h	6 h	12 h	1 day	3 days
Dorsal striatum	WT	6.1 ± 0.6	$7.5 \pm 0.5^{\dagger}$	$8.4 \pm 0.7^{*\ddagger}$	$12 \pm 0.4^{**\ddagger}$	$11.1 \pm 0.8^{**\ddagger}$	$10.0 \pm 0.3^{**\ddagger}$	6.5 ± 0.4
	DYN KO	6.0 ± 0.3	–	–	$15.5 \pm 0.7^{**,\#}$	–	$12.9 \pm 0.3^{**,\#}$	–
NAc	WT	5.0 ± 0.3	5.6 ± 0.5	$6.7 \pm 0.3^{*}$	$6.3 \pm 0.3^{**}$	$7.1 \pm 0.6^{*}$	$6.8 \pm 0.4^{*}$	5.7 ± 0.4
	DYN KO	4.8 ± 0.4	–	–	$11.1 \pm 0.5^{**,\#}$	–	$9.1 \pm 0.5^{**,\#}$	–
Ventral midbrain	WT	5.8 ± 0.4	6.5 ± 0.4	$7.4 \pm 0.3^{*\&}$	$9.7 \pm 0.6^{**\&}$	$8.4 \pm 0.5^{**\&}$	$7.9 \pm 0.4^{**\&}$	6.3 ± 0.5
	DYN KO	5.9 ± 0.6	–	–	$12 \pm 0.6^{**,\#}$	–	$10.2 + 0.4$	–
			B					
Catalase (units/mg protein)		Saline	MA					
			1 h	3 h	6 h	12 h	1 day	3 days
Dorsal striatum	WT	1.7 ± 0.09	$2.0 \pm 0.16^{\dagger}$	$2.1 \pm 0.07^{*,\dagger}$	$2.4 \pm 0.14^{**,\dagger}$	$2.6 \pm 0.19^{**,\ddagger}$	$2.5 \pm 0.13^{**,\ddagger}$	1.9 ± 0.09
	DYN KO	1.6 ± 0.08	–	–	$2.4 \pm 0.06^{**}$	–	$2.2 \pm 0.08^{*}$	–
NAc	WT	$1.4 \pm 0.06^{\&}$	1.5 ± 0.1	$1.6 \pm 0.08^{*}$	1.7 ± 0.08	$1.9 \pm 0.06^{**}$	$1.8 \pm 0.11^{*}$	$1.6 \pm 0.07^{*}$
	DYN KO	1.2 ± 0.05	–	–	$1.8 \pm 0.08^{*}$	–	$1.6 \pm 0.09^{*}$	–
Ventral midbrain	WT	1.6 ± 0.09	1.7 ± 0.32	1.8 ± 0.12	$1.9 \pm 0.09^{*}$	$2.2 \pm 0.13^{**,\&}$	$2.1 \pm 0.11^{**,\&}$	1.8 ± 0.09
	DYN KO	1.3 ± 0.07	–	–	$2 \pm 0.09^{*}$	–	$1.8 \pm 0.09^{*}$	–
			C					
GPx (nmole NADPH/min/mg protein)		Saline	MA					
			1 h	3 h	6 h	12 h	1 day	3 days
Dorsal striatum	WT	$9.9 + 0.3$	8.5 ± 0.8	$7.4 \pm 0.4^{*}$	$4.9 \pm 0.5^{**,\dagger}$	$5.4 \pm 0.3^{**,\dagger}$	$5.6 \pm 0.4^{**,\dagger}$	8.4 ± 0.6
	DYN KO	9.3 ± 0.5	–	–	$3.9 \pm 0.5^{**,\#}$	–	$5.3 \pm 0.4^{**,\#}$	–
NAc	WT	8.7 ± 0.4	8.3 ± 0.3	$7.3 \pm 0.3^{*}$	$6.3 \pm 0.3^{**}$	$6.7 \pm 0.2^{**}$	$7.1 \pm 0.5^{**}$	8.3 ± 0.2
	DYN KO	8.2 ± 0.4	–	–	$4.9 \pm 0.3^{**,\#}$	–	$6.1 \pm 0.4^{**,\#}$	–
Ventral midbrain	WT	9.2 ± 0.6	8.7 ± 0.3	$7.8 \pm 0.5^{*}$	$6.7 \pm 0.3^{**}$	$6.7 \pm 0.5^{**}$	$7.0 \pm 0.4^{**}$	8.6 ± 0.3
	DYN KO	8.9 ± 0.4	–	–	$5.1 \pm 0.5^{**,\#}$	–	$6.3 \pm 0.5^{**,\#}$	–

SOD superoxide dismutase, *GPx* glutathione peroxidase, *Sal* saline, *MA* methamphetamine 35 mg/kg, i.p, *WT* wild-type mice, *DYN KO* prodynorphin knockout mice. Each value is the mean ± SEM of six animals [two-way ANOVA (time points × brain regions) followed by Fisher's LSD pairwise comparisons. Additional two-way ANOVA (time points × gene) with Fisher's LSD pairwise comparisons was done to examine the effect of DYN KO 6 h and 1 day after MA]. $^{*}p < 0.05$, $^{**}p < 0.01$ vs. corresponding Saline. $^{\#}p < 0.05$, $^{\#\#}p < 0.01$ vs. corresponding MA/WT. $^{\dagger}p < 0.05$, $^{\ddagger}p < 0.01$ vs. corresponding NAc or ventral midbrain. $^{\&}p < 0.05$ vs. corresponding NAc

Dang et al. Journal of Neuroinflammation (2018) 15:52
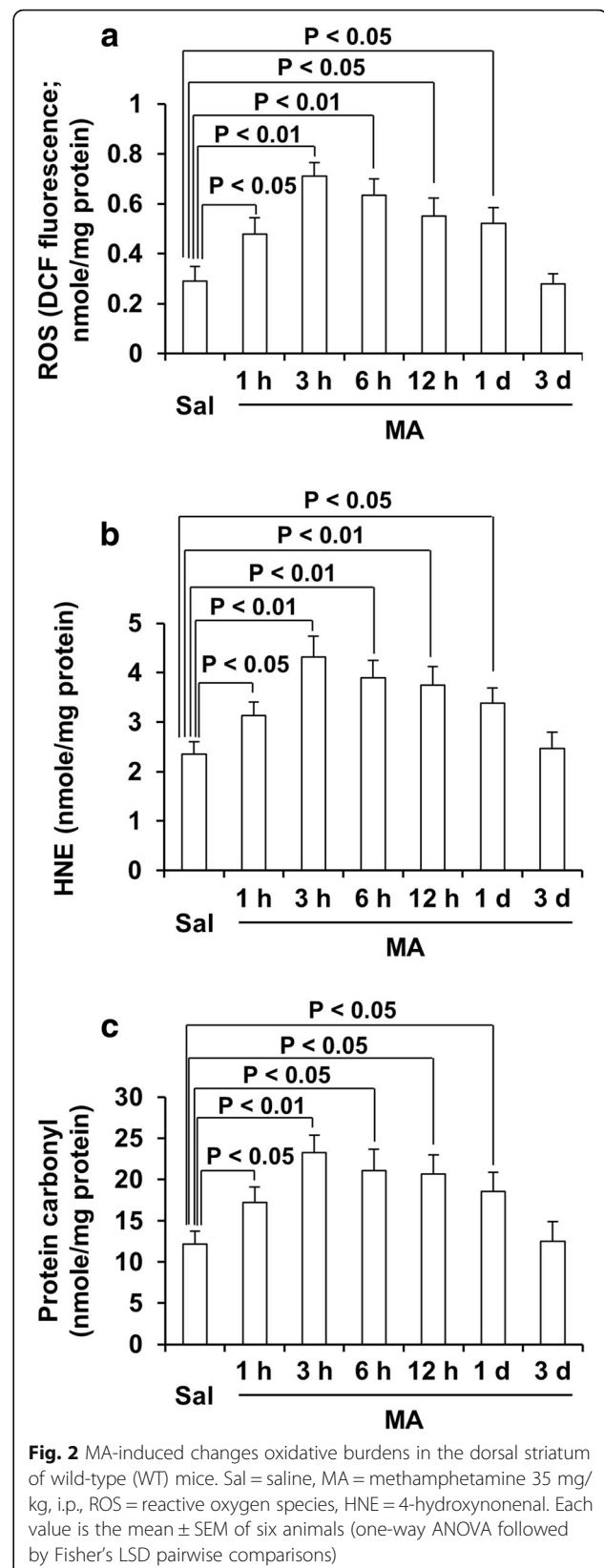
Page 8 of 22

saline) later in WT mice. SOD activity of dorsal striatum (SOD activity 1 h, 3 h, 12 h, or 1 day post-MA; $p < 0.05$ vs. corresponding SOD activity of NAc or ventral midbrain) was significantly higher than that of NAc or ventral midbrain. SOD activity of ventral midbrain (3 h, 6 h, 12 h, or 1 day post-MA; $p < 0.05$ vs. corresponding SOD activity of NAc) was higher than that of NAc (Table 1A). We examined whether genetic depletion of prodynorphin affects enzymatic antioxidants activity induced by MA. Because SOD and GPx activities were significantly changed 6 h post-MA and prodynorphin and substance P mRNA expressions were significantly changed 1 day post-MA, we focused on 6 h and 1 day post-MA.

Prodynorphin knockout significantly potentiated increases in SOD activity 6 h (dorsal striatum, NAc, or ventral midbrain; $p < 0.05$ vs. corresponding brain region of WT mice) and 1 day (dorsal striatum, NAc, or ventral midbrain; $p < 0.01$ vs. corresponding brain region of WT mice. Dorsal striatum; $p < 0.05$ vs. corresponding brain region of prodynorphin knockout mice) after MA treatment in WT mice (Table 1A). Similar to SOD, MA treatment significantly increased catalase activity in WT mice (Table 1B). However, genetic inhibition of prodynorphin did not significantly affect catalase activity of dorsal striatum, NAc, and ventral midbrain of WT mice (Table 1B).

In contrast, treatment with MA resulted in significant decreases in GPx activity 3 h (dorsal striatum, NAc, or ventral midbrain; $p < 0.05$ vs. corresponding saline), 6 h (dorsal striatum, NAc, or ventral midbrain; $p < 0.01$ vs. corresponding saline), 12 h (dorsal striatum, NAc, or ventral midbrain; $p < 0.01$ vs. corresponding saline), and 1 day (dorsal striatum, NAc, or ventral midbrain; $p < 0.01$ vs. corresponding saline) later in WT mice. GPx activity of dorsal striatum (6 h, 12 h, or 1 day post-MA; $p < 0.05$ vs. corresponding GPx activity of NAc or ventral midbrain) was significantly lower than that of NAc and ventral midbrain of MA-treated WT mice (Table 1C). Prodynorphin knockout significantly decreased (dorsal striatum, NAc, or ventral midbrain; $p < 0.05$ vs. corresponding brain region of WT mice) GPx activity 6 h and 1 day post-MA treatment in WT mice (Table 1C).

MA-induced changes oxidative burdens [i.e., reactive oxidative stress (ROS), 4-hydroxynonenal (HNE), and protein carbonyl level] in the dorsal striatum of wild-type (WT) mice

It is well-known that oxidative stress is a key element in MA neurotoxicity [48]. Because dorsal striatum was the most sensitive to MA-induced changes in enzymatic antioxidant as shown in Fig. 2, we focused on dorsal striatum. In our study, parameters of

Fig. 2 MA-induced changes oxidative burdens in the dorsal striatum of wild-type (WT) mice. Sal = saline, MA = methamphetamine 35 mg/kg, i.p., ROS = reactive oxygen species, HNE = 4-hydroxynonenal. Each value is the mean ± SEM of six animals (one-way ANOVA followed by Fisher's LSD pairwise comparisons)

Dang et al. Journal of Neuroinflammation (2018) 15:52

Page 9 of 22

oxidative stress (i.e., ROS, HNE, and protein carbonyl level) were significantly elevated after MA (ROS: 1 h, $p < 0.05$; 3 h, $p < 0.01$; 6 h, $p < 0.01$; 12 h, $p < 0.05$; 1 day, $p < 0.05$. HNE: 1 h, $p < 0.05$; 3 h, $p < 0.01$; 6 h, $p < 0.01$; 12 h, $p < 0.01$; 1 day, $p < 0.05$. Protein carbonyl: 1 h, $p < 0.05$; 3 h, $p < 0.01$; 6 h, $p < 0.05$; 12 h, $p < 0.05$; 1 day, $p < 0.05$), which consistently reached the highest level 3 h post-MA (Fig. 3a–c).

Effects of κ-opioid receptor antagonist nor-binaltorphimine (Nor-B) on the pharmacological activity of ginsenoside Re (GRe) against MA-induced increase in substance P level in WT and prodynorphin KO mice

As shown in Fig. 3a, Nor-B was treated two times before MA administration, and mice received GRe (20 mg/kg, i.p.) for 6 days (5 days before and 1 day after MA). As presented in Fig. 3b, MA-induced decrease ($p < 0.01$ vs. Sal/Sal) in prodynorphin mRNA expression was significantly attenuated ($p < 0.05$) by treatment with GRe. A little substance P-immunoreactivity was observed in the striatum of mice with or without MA (Additional file 1: Figure S2). However, there was a significant induction of substance P-immunoreactivity in the SN of WT mice 1 d post-MA ($p < 0.01$) (Additional file 1: Figure S2). GRe treatment attenuated MA-induced increases in the substance P-immunoreactivity ($p < 0.05$) and substance P mRNA expression ($p < 0.05$) in the SN of mice (Fig. 3c, d). MA-induced increases in substance P levels were more prominent in prodynorphin KO than WT mice ($p < 0.05$). Nor-B (6 mg/kg, i.p.) significantly counteracted GRe-mediated attenuation against substance P-immunoreactivity ($p < 0.05$) or substance P mRNA expression ($p < 0.05$) induced by MA in prodynorphin KO mice (Fig. 3c, d), indicating that GRe requires upregulation of κ-opioid receptor modulation for exerting antioxidant potential.

For more details on Nor-B activity against GRe-mediated effects in WT mice, please refer to Additional file 1: Figure S3.

Effects of neurokinin 1 (NK1) receptor antagonist L-733,060 on κ-opioid receptor antagonist, nor-binaltorphimine (Nor-B)-mediated pharmacological activity in response to antioxidant effects of ginsenoside Re (GRe) against MA insult in the striatum of prodynorphin KO mice

As shown in Fig. 4, oxidative stress (i.e., ROS, HNE, and protein carbonyl level) 3 h post-MA was more evident in prodynorphin KO mice (ROS, HNE, or protein carbonyl level: $p < 0.05$ vs. corresponding WT) than that in WT mice. Nor-B counteracted (ROS, HNE, or protein carbonyl level: $p < 0.05$, respectively) antioxidant effects of GRe in a dose-related manner. L-733,060 inhibited Nor-B-mediated counteraction against the antioxidant effect of GRe in prodynorphin KO mice ($p < 0.05$). In addition, L-733,060 itself attenuated against oxidative stress (ROS, HNE, or protein carbonyl level: $p < 0.05$, respectively) induced by MA. L-733,060 did not exhibit any additive effects in response to GRe-mediated antioxidant effect, suggesting that GRe possesses an interactive pharmacological activity between κ-opioid receptor and NK1 receptor.

The effects of Nor-B on GRe-mediated antioxidant potential in WT mice were shown in Additional file 1: Figure S4.

Substance P-immunoreactivity is expressed in NeuN-immunoreactive neurons, GFAP-immunoreactive astrocytes, or Iba-1-immunoreactive microglial cells in the substantia nigra of WT mice

It was also reported that microglia expresses the substance P gene and NK1 receptor [49]. In order to determine if substance P modulates neuron, astrocyte, and microglia in our experimental system, we conducted double-labeling immunocytochemistry. Substance P-immunoreactivity was co-localized in NeuN-, GFAP-, or Iba-1 immunoreactive cells, suggesting that substance P-immunoreactivity is expressed in neurons, reactive astrocytes, or reactive microglia after MA treatment (Fig. 5).

Effects of neurokinin 1 (NK1) receptor antagonist, L-733,060 on κ-opioid receptor antagonist, nor-binaltorphimine (Nor-B)-mediated pharmacological activity in response to effects of ginsenoside Re (GRe) against changes in NeuN, GFAP, and Iba-1 expression induced by MA in the striatum of prodynorphin KO mice

As presented in Fig. 6a, MA treatment significantly decreased ($p < 0.05$) NeuN expression in both WT and prodynorphin KO mice. GRe, L-733,060, or Nor-B did not significantly alter NeuN expression induced by MA. In contrast, MA tended to increase GFAP expression without reaching statistical analysis in WT mice. However, MA significantly increased ($p < 0.05$) GFAP expression in DYN KO mice. MA-induced increase in GFAP expression was prevented ($p < 0.05$) by L-733,060, but not by GRe (Fig. 6b). Importantly, Iba-1 expression was significantly increased in the striatum 1 day after MA ($p < 0.05$). MA-induced increase in Iba-1 expression was more evident ($p < 0.05$) in prodynorphin KO than in WT mice. Either GRe ($p < 0.05$) or L-733,060 ($p < 0.05$) significantly attenuated MA-induced increase in Iba-1 expression. Treatment of L-733,060 did not exhibit any additional effects in response to the pharmacological activity of GRe. Nor-B (6 mg/kg, i.p.) counteracted ($p < 0.05$) against GRe-mediated attenuation in Iba-1 expression. L-733,060 treatment inhibited ($p < 0.05$) Nor-B-induced counteraction (Fig. 6a). This phenomenon consistently paralleled Iba-1-immunoreactivity (Iba-1-IR), indicating that
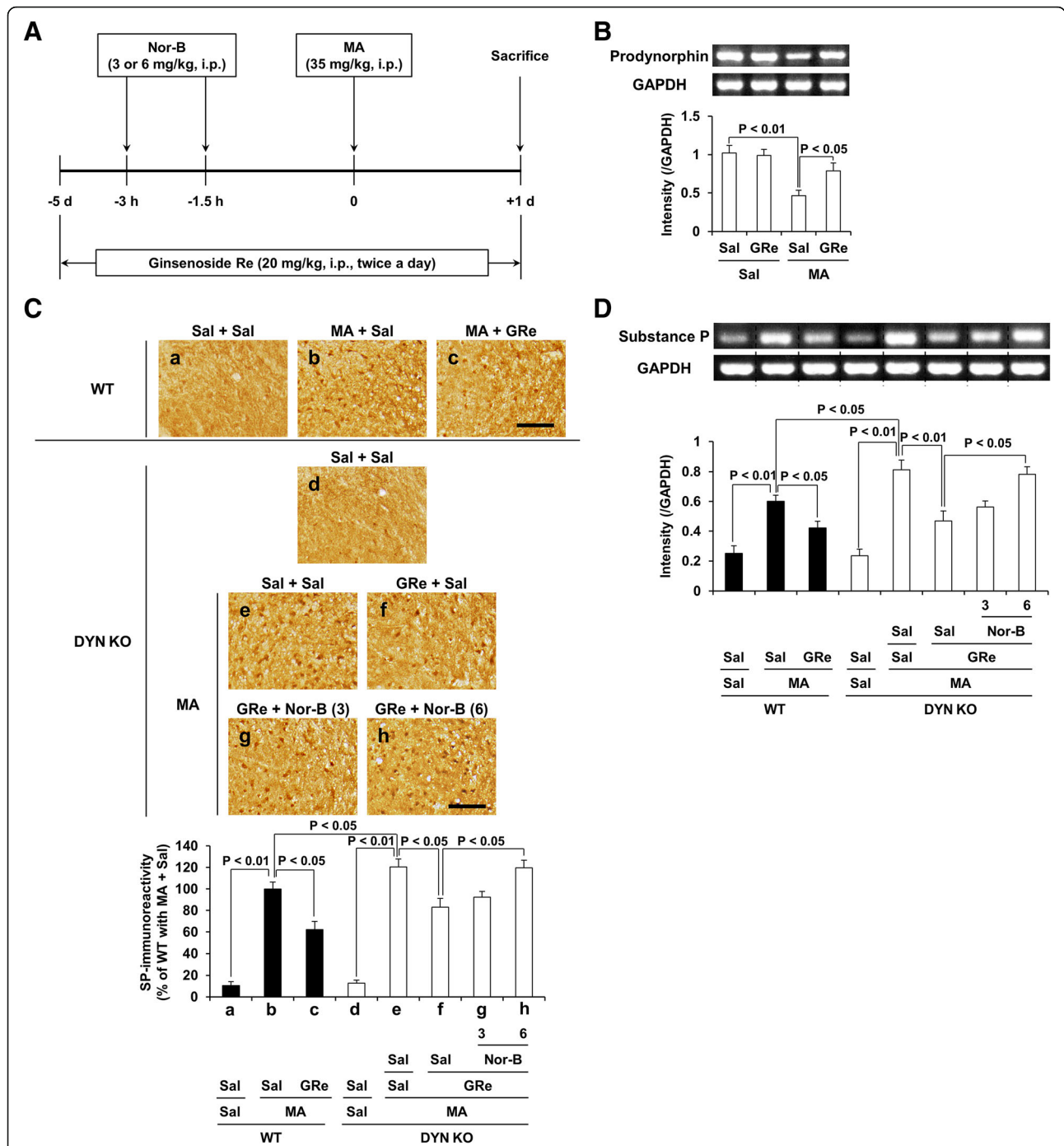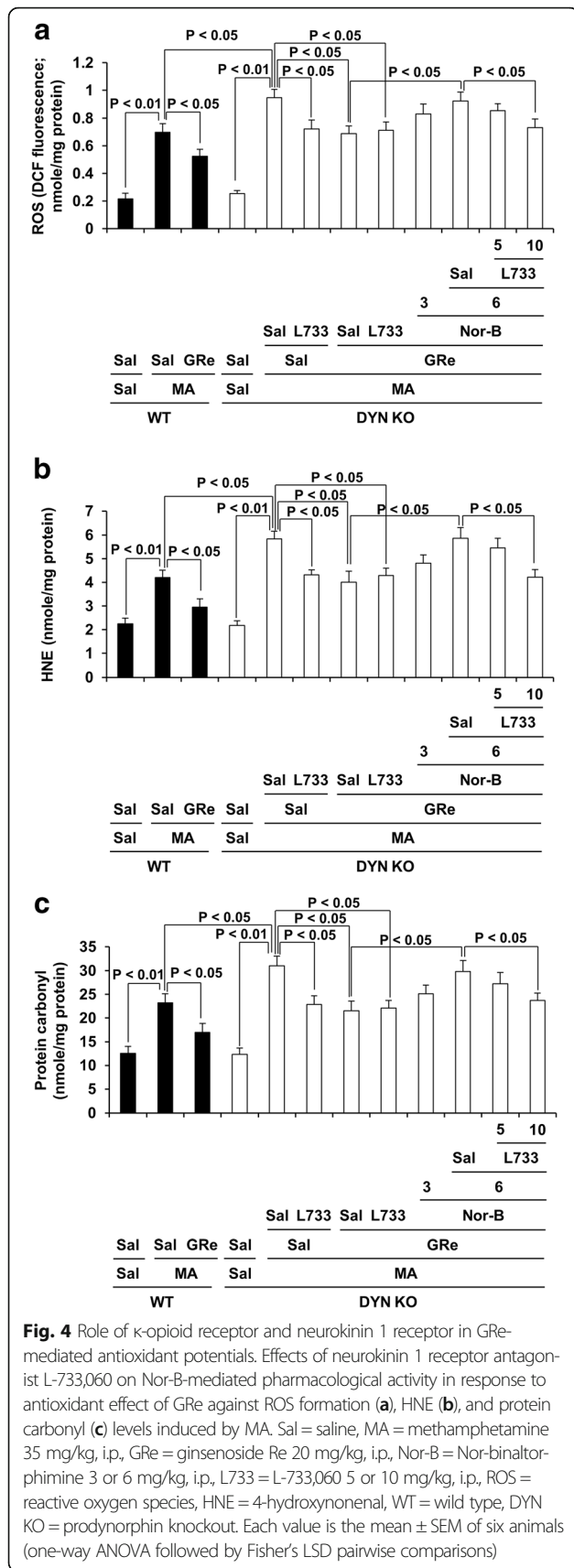
Dang *et al. Journal of Neuroinflammation* (2018) 15:52

Page 10 of 22

Fig. 3 Role of κ-opioid receptor in GRe-mediated modulation of prodynorphin and substance P. Experimental design for determining whether κ-opioid receptor is involved in GRe-mediated effects against dopaminergic toxicity induced by MA; mice received Nor-B by two times (3 and 1.5 h) before MA treatment. Mice received ginsenoside Re twice a day for seven consecutive days (i.e., 5 days before and 1 day after MA) (**a**). Effect of GRe on MA-induced decrease in prodynorphin mRNA expression in the striatum of mice (**b**). Effects of κ-opioid receptor antagonist Nor-B on GRe-mediated pharmacological activity against MA-induced increases in substance P (SP)-immunoreactivity (**c**) and substance P mRNA expression (**d**) in the substantia nigra (SN) of DYN KO mice. Sal = saline, MA = methamphetamine 35 mg/kg, i.p., GRe = ginsenoside Re 20 mg/kg, i.p., Nor-B = nor-binaltorphimine 3 or 6 mg/kg, i.p., WT = wild-type mice, DYN KO = prodynorphin knockout. Each value is the mean ± SEM of six animals [two-way ANOVA (B) or one-way ANOVA (C and D) followed by Fisher's LSD pairwise comparisons]. Scale bar = 100 μm

Dang et al. Journal of Neuroinflammation (2018) 15:52

Page 11 of 22

Fig. 4 Role of κ-opioid receptor and neurokinin 1 receptor in GRe-mediated antioxidant potentials. Effects of neurokinin 1 receptor antagonist L-733,060 on Nor-B-mediated pharmacological activity in response to antioxidant effect of GRe against ROS formation (**a**), HNE (**b**), and protein carbonyl (**c**) levels induced by MA. Sal = saline, MA = methamphetamine 35 mg/kg, i.p., GRe = ginsenoside Re 20 mg/kg, i.p., Nor-B = Nor-binaltor-phimine 3 or 6 mg/kg, i.p., L733 = L-733,060 5 or 10 mg/kg, i.p., ROS = reactive oxygen species, HNE = 4-hydroxynonenal, WT = wild type, DYN KO = prodynorphin knockout. Each value is the mean ± SEM of six animals (one-way ANOVA followed by Fisher's LSD pairwise comparisons)

western blotting analysis (Fig. 6c) supports immuno-staining (Fig. 6d). As shown in Additional file 1: Figure S5, MA-induced Iba-1-immunoreactive microglial cells were more pronounced in the striatum than in the SN. For more details on the effects of Nor-B on the protective activity of GRe against microglial activation induced by MA in WT mice, please refer to Additional file 1: Figure S6.

Effects of neurokinin 1 (NK1) receptor antagonist L-733,060 on κ-opioid receptor antagonist nor-binaltorphimine (Nor-B)-mediated pharmacological activity in response to effects of ginsenoside Re (GRe) against pro-apoptotic changes induced by MA in the striatum of prodynorphin KO mice

Cadet and colleagues [50] made the first in vivo demonstration that a neurotoxic dose of MA causes differential regulation of several Bcl-2 family genes with two distinct clustering consisting of upregulation of pro-death and downregulation of anti-death gene expression. Their results brought further highlight the role that pro-apoptotic cell death plays an important role in MA neurotoxicity [51–57].

As presented in Fig. 7a, b, MA treatment significantly increased Bax ($p < 0.01$) and cleaved caspase-3 ($p < 0.01$) expression in WT mice. MA-induced Bax and cleaved caspase-3 expression was more evident ($p < 0.05$, respectively) in prodynorphin KO mice than in WT. GRe or L-733,060 attenuated MA-induced increase in Bax ($p < 0.05$) and cleaved caspase-3 ($p < 0.05$) expression in prodynorphin KO mice. Consistently, MA significantly decreased ($p < 0.01$) Bcl-2 expression (Fig. 7c). This decrease was more pronounced in prodynorphin KO ($p < 0.05$) than in WT mice, which was significantly attenuated by treatment with GRe ($p < 0.05$) or L-733,060 ($p < 0.05$). L-733,060 did not produce any additional effect against the anti-apoptotic potential mediated by GRe. The attenuation by GRe was significantly counteracted ($p < 0.05$) by Nor-B (6 mg/kg, i.p.), which was subsequently inhibited ($p < 0.05$) by L-733,060 (10 mg/kg, i.p.).

The effects of Nor-B on the protective activity of GRe against MA-induced apoptotic changes in WT were presented in Additional file 1: Figure S7.

Effects of genetic depletion of prodynorphin on MA-induced changes in dopamine and dopamine turnover rate in the dorsal striatum, nucleus accumbens (NAc), and ventral midbrain of mice

As shown in Fig. 8a–c, we investigated whether prodynorphin knockout affects MA-induced dopaminergic impairments in mice. MA-induced significant decreases in dopamine level was observed in dorsal striatum ($p < 0.01$ vs. saline), NAc ($p < 0.05$ vs. saline),
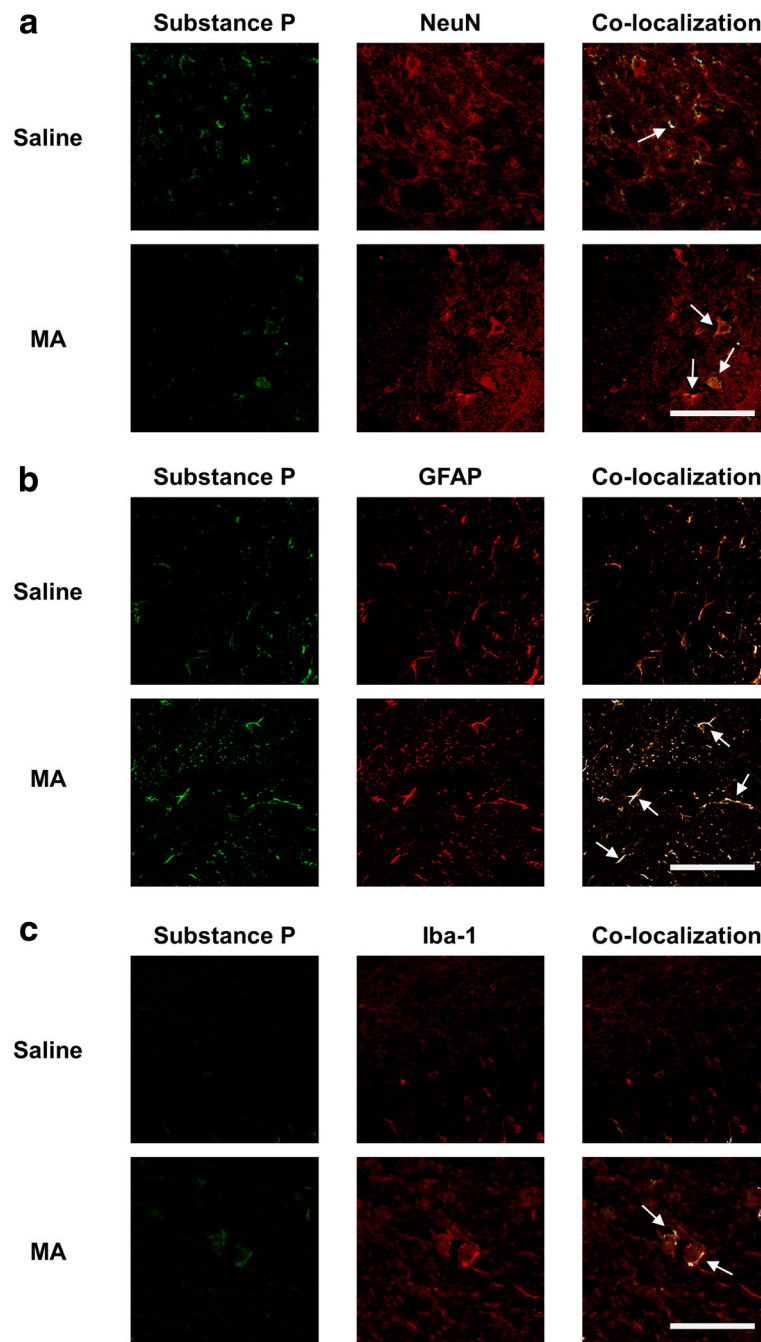
Dang et al. Journal of Neuroinflammation (2018) 15:52

Page 12 of 22

Fig. 5 MA-induced changes in substance P-immunodistribution. Substance P-immunoreactivity was localized in the NeuN-labeled neurons (**a**), GFAP-labeled astrocytes (**b**), and Iba-1-labeled microglial cells (**c**). Arrow indicates co-localization. Scale bar = 100 μm

and ventral midbrain ($p < 0.01$ vs. saline) in WT mice. MA-induced dopamine loss was more pronounced ($p < 0.05$ vs. WT) than in the dorsal striatum of prodynorphin knockout mice. However, prodynorphin knockout did not significantly affect MA-induced dopaminergic loss in NAc and ventral midbrain. Consistently, MA-induced dopamine turnover rate was significantly increased in dorsal striatum, NAc, and ventral midbrain in WT and prodynorphin knockout mice. Dopamine turnover rate was higher in the dorsal striatum of MA-treated prodynorphin knockout ($p < 0.05$) than WT mice. However, prodynorphin knockout did not significantly change dopamine turnover rate of NAc and ventral midbrain in mice. Thus, we focused on dorsal striatum for the mechanistic study on dopaminergic system.
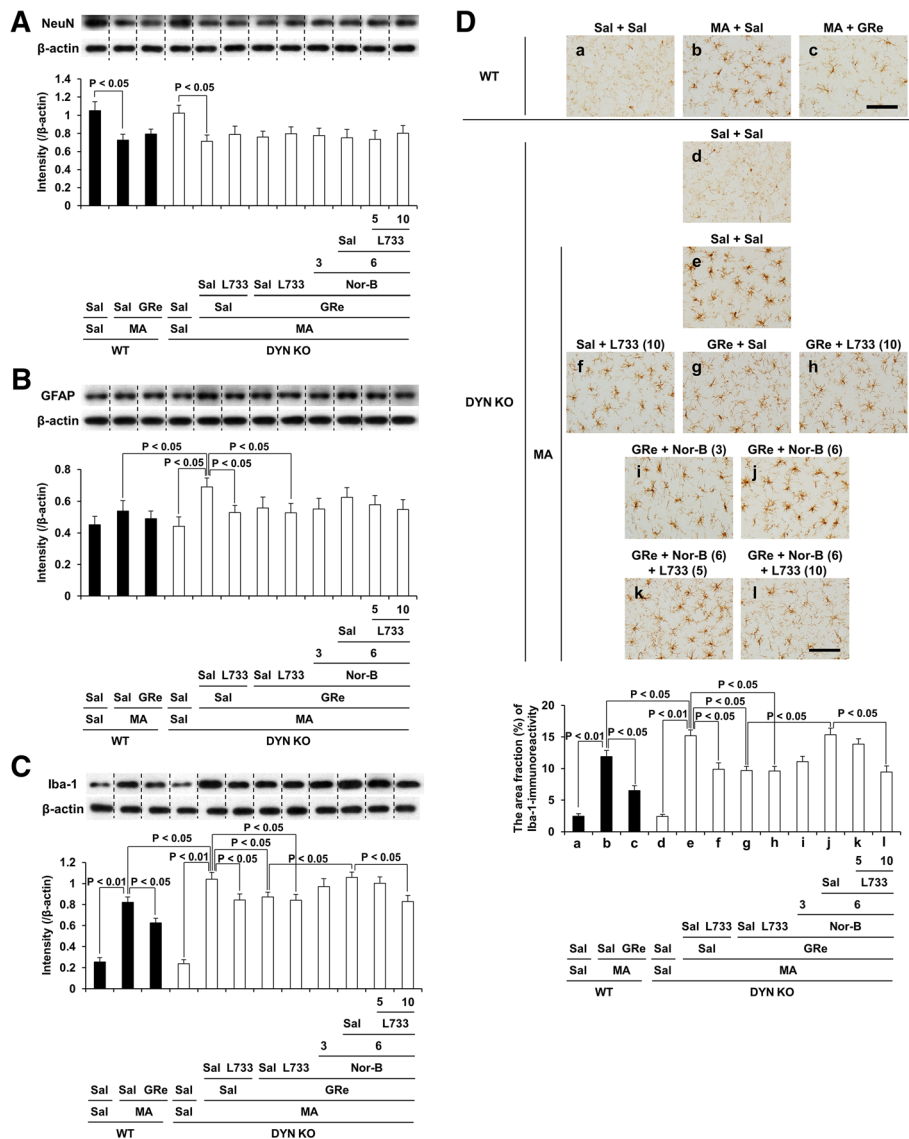
Dang et al. Journal of Neuroinflammation (2018) 15:52

Page 13 of 22

Fig. 6 Role of κ-opioid and neurokinin 1 receptors in GRe-mediated neuronal, astrocytic, and microglial modulation. Effects of neurokinin 1 receptor antagonist L-733,060 on κ-opioid receptor antagonist Nor-B-mediated pharmacological activity in response to effects of GRe against the changes in NeuN (**a**), GFAP (**b**), Iba-1 expression (**c**), and Iba-1-immunoreactivity (**d**) induced by MA in the striatum of DYN KO mice. Sal = saline, MA = methamphetamine 35 mg/kg, i.p., GRe = ginsenoside Re 20 mg/kg, i.p., Nor-B = Nor-binaltorphimine 3 or 6 mg/kg, i.p., L733 = L-733,060 5 or 10 mg/kg, i.p., GFAP = glial fibrillary acidic protein, Iba-1 = ionized calcium-binding adapter molecule 1, WT = wild type, DYN KO = prodynorphin knockout. Each value is the mean ± SEM of six animals (one-way ANOVA followed by Fisher's LSD pair-wise comparisons). Scale bar = 100 μm

Effects of neurokinin 1 (NK1) receptor antagonist L-733,060 on κ-opioid receptor antagonist nor-binaltorphimine (Nor-B)-mediated pharmacological activity in response to effects of ginsenoside Re (GRe) against dopaminergic impairments induced by MA in the dorsal striatum of prodynorphin KO mice

MA-induced decrease ($p < 0.01$) in TH-immunoreactivity (TH-IR) of WT mice. This decrease was more pronounced ($p < 0.05$) in prodynorphin KO mice than in WT mice (Fig. 9a and Additional file 1: Figure S8). This

decrease in prodynorphin KO mice was significantly protected by treatment with GRe ($p < 0.05$) or L-733,060 ($p < 0.05$). L-733,060 did not exhibit any additive effects against neuroprotective effects of GRe. Nor-B (6 mg/kg, i.p.) significantly counteracted ($p < 0.01$) the protective effects of GRe. Counteraction by Nor-B was significantly inhibited ($p < 0.01$) by L-733,060 (10 mg/kg, i.p.). Result of TH-IR paralleled that of TH expression and dopamine level, respectively (Fig. 9b, c). Consistently, increase ($p < 0.05$) in dopamine turnover rate was more
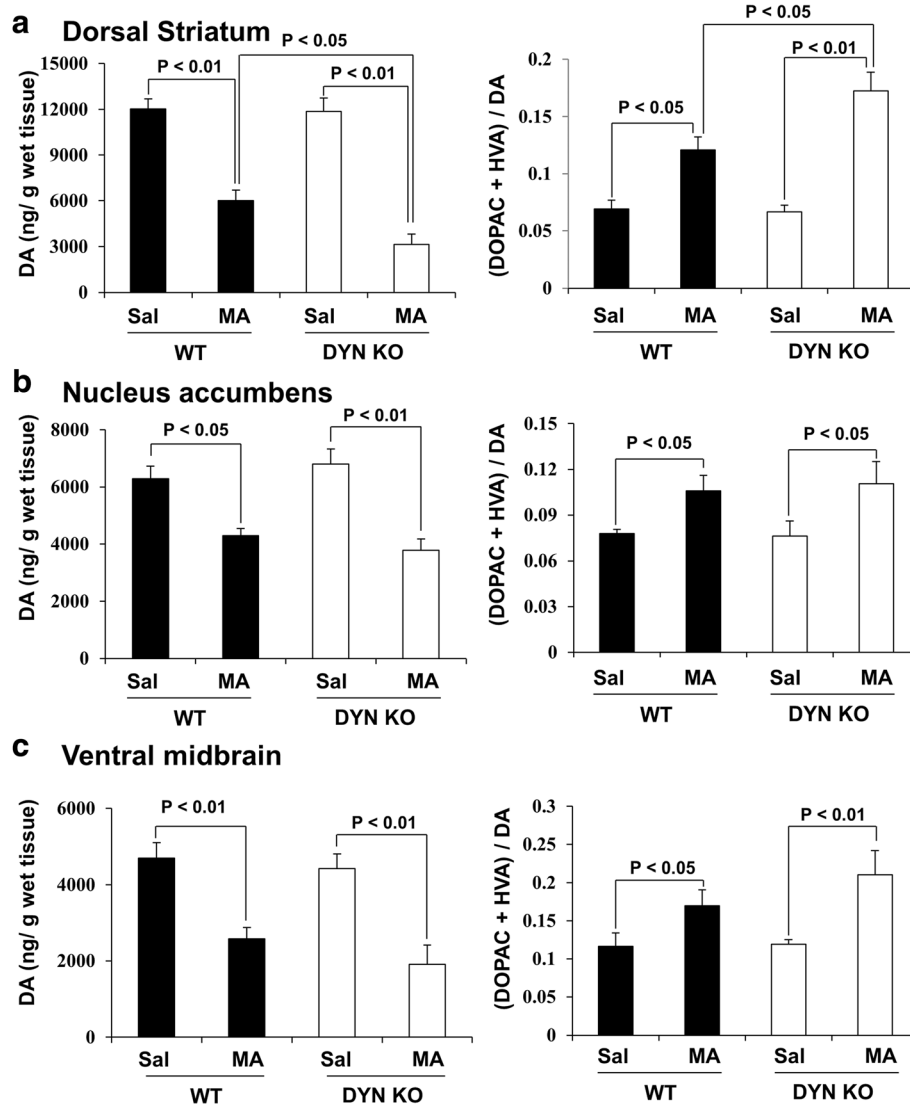
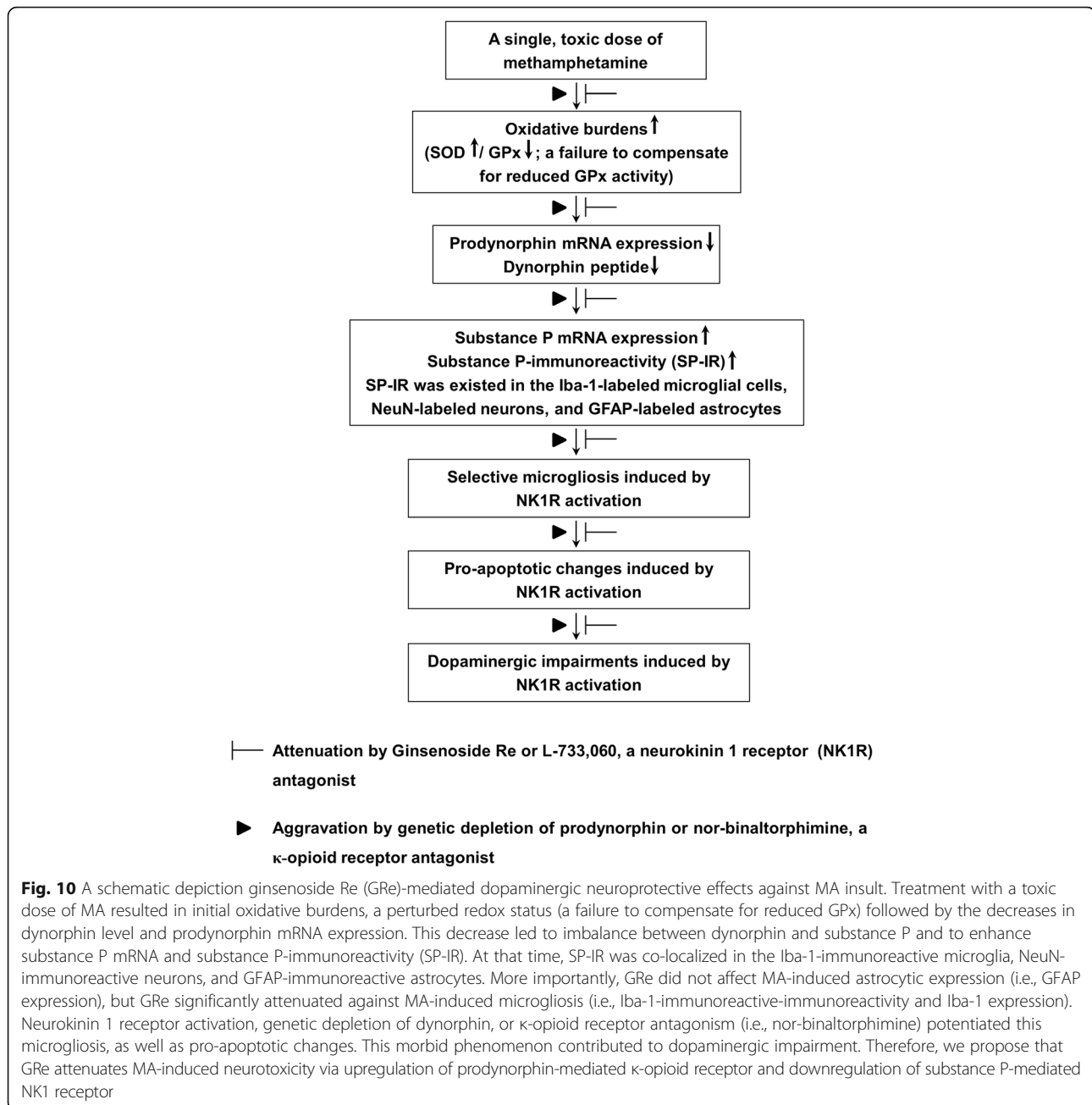Dang *et al. Journal of Neuroinflammation* (2018) 15:52

Page 14 of 22

Fig. 7 Role of κ-opioid and neurokinin 1 receptors in GRe-mediated anti-apoptotic potentials. Effects of neurokinin 1 receptor antagonist L-733,060 on κ-opioid receptor antagonist Nor-B-mediated pharmacological activity in response to effects of GRe against the changes in Bax (**a**), cleaved caspase-3 (**b**), and Bcl-2 expression (**c**) induced by MA in the striatum of DYN KO mice. Sal = saline, MA = methamphetamine 35 mg/kg, i.p., GRe = ginsenoside Re 20 mg/kg, i.p., Nor-B = Nor-binaltorphimine 3 or 6 mg/kg, i.p., L733 = L-733,060 5 or 10 mg/kg, i.p., WT = wild type, DYN KO = prodynorphin knockout. Each value is the mean ± SEM of six animals (one-way ANOVA followed by Fisher's LSD pairwise comparisons)

pronounced in prodynorphin KO than in WT mice. Although GRe or L-733,060 attenuated this increase ($p < 0.05$), L-733,060 did not show any additional effects against dopaminergic neuroprotective activity of GRe. Nor-B treatment significantly counteracted ($p < 0.05$) neuroprotective effects of GRe. L-733,060 treatment inhibited ($p < 0.05$) against the counteraction induced by Nor-B (Fig. 9d).

The effects of Nor-B on the protective activity of GRe against dopaminergic impairments induced by MA in WT were shown in Additional file 1: Figure S9.

Discussion

Accumulating evidence has suggested that the positive effects of GRe may be due to its antioxidant and anti-inflammatory activities [30, 58]. Similarly, we observed that endogenous dynorphin plays a critical role in protecting dopaminergic neurons through its anti-inflammatory effects [3]. Here, we found that GRe modulated positive interaction between dynorphin and substance P to suppress oxidative stress and pro-inflammatory responses induced by MA. In line with previous reports [6, 7], we observed that NK1 receptor antagonism attenuated against MA-induced dopaminergic toxicity. However, NK1 receptor antagonist L-733,060 did not show any additional positive effect against neuroprotective activity by GRe, indicating that NK1 receptor is also one of the molecular pharmacological targets for GRe-mediated neuroprotective activity. Our result may be in line with a previous finding [23] that interaction between dynorphin and substance P is critical for modulating dopaminergic neurotoxicity. GRe treatment significantly attenuated MA-induced oxidative burdens, microglial activation, pro-apoptotic changes, and dopaminergic impairments via positive modulation between dynorphin-mediated κ-opioid receptor and substance P-mediated NK1 receptor (Fig. 10).

In this study, we selected a neurotoxic model induced by MA (35 mg/kg, i.p.), because this acute toxic model efficiently induces neuronal pro-apoptosis in the mouse striatum [53, 59]. Our recent reports indicated that a single, high dose of MA selectively induces proapoptosis

Dang *et al. Journal of Neuroinflammation* (2018) 15:52

Page 15 of 22

Fig. 8 Effects of genetic depletion of DYN on MA-induced dopaminergic change. **a** Effects of dorsal striatum. **b** Effects of nucleus accumbens. **c** Effects of ventral midbrain. Sal = saline, MA = methamphetamine 35 mg/kg, i.p., GRe = ginsenoside Re 20 mg/kg, i.p., Nor-B = Nor-binaltorphimine 3 or 6 mg/kg, i.p., L733 = L-733,060 5 or 10 mg/kg, i.p., WT = wild type, DYN KO = prodynorphin knockout. Each value is the mean ± SEM of six animals (two-way ANOVA followed by Fisher's LSD pairwise comparisons)

in the striatum of mice [55, 60]. This range of MA dose also induces the loss of striatal dopamine terminal markers, such as dopamine transporter, tyrosine hydroxylase, and tissue dopamine content [61–63].

Dynorphin is the major posttranslational product of the prodynorphin gene and the presumed endogenous ligand for the κ-opioid receptor [34]. El Daly et al. [64] found that the systemic administration of a selective κ-opioid receptor agonist U69593 attenuated reduction in presynaptic dopamine neuronal function in response to repeated methamphetamine administration. Consistently, our finding indicated that κ-opioid receptor plays a protective role in dopaminergic neurodegeneration induced by a toxic dose of MA. κ-opioid receptor

activation attenuates the initiation and long-term expression of sensitization to the locomotor-activating effects of cocaine [65–68]. Earlier studies have shown that κ-opioid receptor agonists modulate dopaminergic neurotransmission in the SN, neostriatum, and the mesolimbic system [69–72]. Administration of dynorphin (1–13), the postulated endogenous ligand for the κ-opioid receptor, also attenuated the development of D-amphetamine-induced behavioral sensitization [73]. Therefore, it is possible that κ-opioid receptor agonist might be important for positive dopaminergic modulation.

In this study, treatment with MA resulted in significant and constant increases in SOD activity in the dorsal

Dang et al. Journal of Neuroinflammation (2018) 15:52

Page 16 of 22
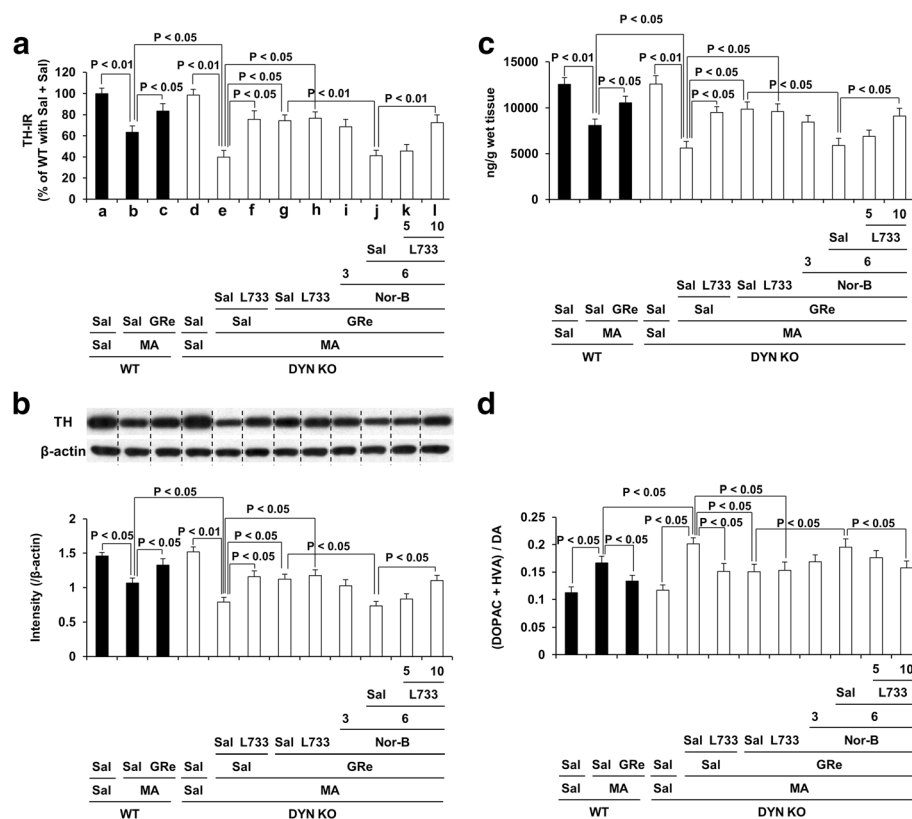
Fig. 9 Role of κ-opioid and neurokinin 1 receptors in GRe-mediated dopaminergic neuroprotection. Effects of neurokinin 1 receptor antagonist L-733,060 on κ-opioid receptor antagonist Nor-B-mediated pharmacological activity in response to effects of GRe against changes in tyrosine hydroxylase-immunoreactivity (TH-IR; **a**), TH expression (**b**), dopamine level (**c**), and dopamine turnover rate (**d**) induced by MA in the striatum of DYN KO mice. Sal = saline, MA = methamphetamine 35 mg/kg, i.p., GRe = ginsenoside Re 20 mg/kg, i.p., Nor-B = Nor-binaltorphimine 3 or 6 mg/kg, i.p., L733 = L-733,060 5 or 10 mg/kg, i.p., WT = wild type, DYN KO = prodynorphin knockout. Each value is the mean ± SEM of six animals (one-way ANOVA followed by Fisher's LSD pairwise comparisons)

striatum (> ventral midbrain > NAc) of mice, but did not involve a concomitant increase in GPx activity. Increased SOD activity can lead to an accumulation of H_2O_2, which in the absence of simultaneous increases in the activity of GPx, could increase Fenton reactions leading to the stimulation of ROS and lipid peroxidation/protein oxidation that result in irreversible cellular damage [74, 75]. In contrast, increased catalase activity in MA-treated wild-type mice could be an adaptive response to higher levels of H_2O_2 generated by inhibition of GPx activity, the brain has low-level catalase activity and only moderate amounts of SOD and GPx [75, 76]. Our observation of increased ROS, and lipid peroxidation/protein oxidation products implies that GPx activity, rather than increased SOD, modulates these endpoints. Furthermore, significant elevation of SOD activity in the early stages of MA insult in mice could be a response to the enhanced superoxide generated during MA-induced neurotoxicity [43, 77]. In other words, increased activity of SOD as well as decreased GPx activity in prodynorphin KO mice may be responsible for

accumulating H_2O_2 levels, which could activate oxidative burdens. Therefore, the protective effect against MA-induced dopaminergic deficits in the presence of GRe might reflect an upregulation of dynorphin/ κ-opioid receptor as well as down-regulation of substance P/NK1 receptor.

GRe exerts an antioxidant potential, mitochondrial restoration, and anti-apoptosis via protein kinase C δ (PKCδ) inhibition in SH-SY5Y human neuroblastoma cells [58]. Shin et al. [30] also demonstrated that GRe rescued MA-induced oxidative damage, mitochondrial dysfunction, microglial activation, and dopaminergic degeneration by inhibiting PKCδ gene in mice. Previous studies have reported that substance P facilitated the phosphorylation of PKCδ in rat parotid acinar cells [78]. Moreover, it has been reported that PKCδ plays an important role in substance P-induced pro-inflammatory signaling in human colonocytes [79]. Substance P-induced PKCδ activation and its downstream signaling pathway are dependent on NK1 receptor [80]. Wang et al. [15] also identified PKCδ as a downstream signal

Dang *et al. Journal of Neuroinflammation* (2018) 15:52

Page 17 of 22

Fig. 10 A schematic depiction ginsenoside Re (GRe)-mediated dopaminergic neuroprotective effects against MA insult. Treatment with a toxic dose of MA resulted in initial oxidative burdens, a perturbed redox status (a failure to compensate for reduced GPx) followed by the decreases in dynorphin level and prodynorphin mRNA expression. This decrease led to imbalance between dynorphin and substance P and to enhance substance P mRNA and substance P-immunoreactivity (SP-IR). At that time, SP-IR was co-localized in the Iba-1-immunoreactive microglia, NeuN-immunoreactive neurons, and GFAP-immunoreactive astrocytes. More importantly, GRe did not affect MA-induced astrocytic expression (i.e., GFAP expression), but GRe significantly attenuated against MA-induced microgliosis (i.e., Iba-1-immunoreactive-immunoreactivity and Iba-1 expression). Neurokinin 1 receptor activation, genetic depletion of dynorphin, or κ-opioid receptor antagonism (i.e., nor-binaltorphimine) potentiated this microgliosis, as well as pro-apoptotic changes. This morbid phenomenon contributed to dopaminergic impairment. Therefore, we propose that GRe attenuates MA-induced neurotoxicity via upregulation of prodynorphin-mediated κ-opioid receptor and downregulation of substance P-mediated NK1 receptor

that bridges substance P-mediated NK1 receptor activation and NOX2 activation in microglia. Therefore, it is plausible that GRe modulates molecular interaction between substance P and PKCδ against MA insult.

Substance P is considered the prototype of the tachykinin family and is encoded by the pre-protachykinin-A gene. Substance P is the natural ligand that displays the highest affinity for the NK1 receptor [6]. Earlier studies have found that multiple administrations of MA elevated the levels of pre-protachykinin-A mRNA and substance P within striatonigral neurons, suggesting that exposure to MA augments tachykinin neurotransmission in the

striatonigral pathway [81–83]. High levels of substance P are present in the SN, where it binds to NK1 receptors expressed on dopaminergic neurons [5]. Consistently, we observed that treatment with MA resulted in a significant increase in substance P-immunoreactivity. Previous research indicated that substance P binding at NK1 receptors expressed on microglia and astrocytes may directly result in the activation of these glial cells in the central nervous system [84, 85].

In this study, we observed that substance P localized with neurons, astrocytes, or microglia after MA treatment. In addition, treatment with MA resulted in

Dang et al. Journal of Neuroinflammation (2018) 15:52

Page 18 of 22

increases in GFAP and Iba-1 expression. The increase in Iba-1 expression was attenuated by GRe or NK1 receptor antagonist L-733,060, which was consequently counteracted by κ-opioid receptor antagonist Nor-B. However, L-733,060, but not GRe, affected GFAP expression induced by MA. This finding supported previous study [15], suggesting that signaling events mediated by GRe, dynorphin, or substance P are specific to microglial cells.

Earlier study indicated that substance P and dynorphin co-exist extensively in specific populations of striatal projection neurons, indicating a correlation between two peptides [86]. Endogenous substance P potentiates immunological activation of microglia induced by lipopolysaccharide (LPS) or MPTP in the SN, suggesting the critical role of substance P as an inflammatory mediator in dopaminergic neurodegeneration [13, 14]. Block et al. [23] demonstrated a tightly regulated mechanism governing microglia-derived oxidative stress, in which the neuropeptide balance of dynorphin and substance P is critical to dopamine neuron survival. Substance P (10^{-13}–10^{-14} M) is selectively toxic to dopaminergic neurons in the presence of microglia, which was significantly protected by dynorphin. In line with previous research [23], here, we proposed that the interaction between dynorphin and substance P may be essential for modulating dopaminergic toxicity induced by a single, high dose of MA (35 mg/kg, i.p.), indicating critical roles of κ-opioid receptor and NK1 receptor in modulating microglial activation.

Dopaminergic neurons in the SN are more susceptible to oxidative and inflammatory insults than neurons in other regions [87–90]. This phenomenon may be related to a higher density of microglia in SN than in other brain regions [91]. Similarly, a strong substance P-like immunoreactivity [92–94] has been shown in SN, and substance P is considered a likely neurotransmitter [95] which excites neurons in SN [96]. Wang et al. [15] proposed that substance P released from the nerve terminal of striatonigral projections may contribute to the higher microglial densities in the SN through the induction of proliferation and/or through chemotaxic recruitment of microglia. This is because the disproportionately higher density of microglia and potential substance P itself in the SN may contribute to the increased susceptibility of nigral dopaminergic neurons to regional neuroinflammation [91, 97].

It has been well-recognized that macrophages/microglia play different roles in tissue repair or damage in response to CNS injury. Microglia in the brain have classically activated M1 phenotype or alternatively activated M2 phenotype, depending on the inflammatory conditions of the local microenvironment. MA treatment enhanced the mRNA expression of M1 markers (CD16, CD32, and CD86), while those of M2 markers (arginase 1 and CD206) were decreased [3]. Endogenous dynorphin depletion accelerated microglial differentiation to the M1 phenotype after MA, suggesting that dynorphin may serve to dampen this neuroinflammatory process [3]. Importantly, treatment with GRe resulted in a significant attenuation against MA-induced increase in mRNA expression of M1 markers, indicating that GRe possesses an anti-inflammatory effect [30].

Microgliosis has been traditionally considered to play a passive role in the removal of dead or damaged neurons and debris by phagocytosis [3]. However, it is clear that microglial cells are reactivated during microgliosis, and further exacerbate neurodegeneration under severe inflammatory conditions [3]. It could be speculated that the balance between dynorphin and substance P appears to be critical for microglial activation and long-term survival of nigrostriatal dopaminergic neurons [23, 98]. Parallel with inducing microgliosis, MA can cause neuronal proapoptosis, in addition to terminal degeneration, by increasing caspase activity [55, 60, 99], current study].

Our earlier in vitro studies [98, 100] did not support our current in vivo study. Kong et al. [100] demonstrated that ultra-low concentrations (10^{-12}–10^{-16} M) of dynorphin A-(1–8) significantly inhibited the LPS-induced production of NO or TNF-α in mixed glia cultures. The inhibitory effects of dynorphin A-(1–8) were not blocked by κ-opioid receptor antagonist Nor-B. Similarly, LPS-induced neurotoxicity in rat midbrain neuron-glia cultures was significantly reduced by treatment with ultra-low concentrations (10^{-13}–10^{-15} M) of dynorphin A (1–17), but not by U50488, a synthetic κ-opioid receptor agonist [98], suggesting that dynorphin-mediated protective activity in vitro is not dependent on κ-opioid receptor. This disparity between our in vivo finding and previous in vitro reports remains to be fully elucidated.

It is well known that NAc is more resistant to MA toxicity [101], but the mechanism underlying the regional heterogeneity of MA has not yet been fully elucidated. The dopamine transporter (DAT) is believed to be an essential component of pathway leading to MA neurotoxicity in the striatum [102]. Supporting this notion, the basal level of DAT binding sites is higher in striatum than in NAc [6]. In addition, it was reported that a toxic dose of MA caused the delayed increase of glutamate release only in the striatum (caudate putamen), but not in the NAc [103]. A single injection of amphetamine or MA increased mRNA levels of preprotachykinin-A, along with preproenkephalin and preprodynorphin (encoding the neuropeptides substance P, enkephalines, and dynorphin, respectively) in the neostriatum with far greater elevation in caudate

Dang *et al. Journal of Neuroinflammation* (2018) 15:52

Page 19 of 22

putamen than in NAc [104, 105], suggesting the differential actions of peptide systems to MA in brain regions. Observed regional differences between the caudate putamen and the NAc may reflect the existence of different mechanisms of MA-induced toxicity operating in these brain regions [6]. In addition, if nigrostriatal degeneration had occurred, MA treatment might activate microglial activation in the SN. However, MA-induced microglial activation in SN was much less than in striatum (Additional file 1: Figure S5), suggesting that MA-induced striatal burdens did not progress to ventral midbrain. It was demonstrated that the extent of toxicity within the ventral midbrain was greater in the SN pars compacta then in the reticulate and ventral tegmental area [106]. Rather, it is likely that the preservation of cellular integrity of ventral midbrain is a critical factor that allows for the recovery of the dopaminergic system [107]. Consistently, whole ventral midbrain is also resistant to MA toxicity in our experimental condition (please refer to Table 1, Fig. 8, and Additional file 1: Figure S1).

GRe is a main ginsenoside and an important ingredient in ginseng leaf, berry, and root [24, 35, 36, 108]. Ginseng root has been mainly used as herbal medicine, whereas other parts have been considered by-products or minor products. Earlier reports indicated that GRe is more abundant in the leaf, berry, and flower bud than in the root [35, 36, 109], reflecting possible pharmacoeconomical advantages of GRe in terms of developing natural/drug resources.

Conclusions

Our findings suggest that GRe exerts antioxidant, antiinflammatory, and anti-apoptotic potentials against MA-induced dopaminergic neurotoxicity, and that interactive modulation between dynorphin and substance P is essential for GRe-mediated dopaminergic neuroprotection. The promising efficacy of GRe in response to MA insult may be helpful for developing therapeutic interventions for disorders of dopaminergic degeneration, although additional evidence should be obtained.

Additional files

Additional file 1: Figure S1. MA-induced changes in dynorphin level in nucleus accumbens (NAc) and ventral midbrain in mice. **Figure S2.** MA-induced changes in substance P immunodistribution in the striatum and substantia nigra. **Figure S3.** Role of κ-opioid receptor in GRe-mediated modulation in substance P mRNA expression. **Figure S4.** Role of κ-opioid receptor in GRe-mediated antioxidant potentials. **Figure S5.** MA-induced changes in Iba-1 immunoreactive microglial cells in the striatum and substantia nigra. **Figure S6.** Role of κ-opioid receptor in GRe-mediated anti-microglial potentials. **Figure S7.** Role of κ-opioid receptor in GRe-mediated anti-apoptotic potentials. **Figure S8.** Role of κ-opioid and neurokinin 1 receptors in GRe-mediated attenuation on the loss of TH-immunoreactivity (TH-IR). **Figure S9.** Role of κ-opioid receptor in GRe-mediated dopaminergic neuroprotection. (DOCX 18 kb)

Author details

[1]Neuropsychopharmacology and Toxicology Program, College of Pharmacy, Kangwon National University, Chunchon 24341, Republic of Korea. [2]Department of Anatomy and Cell Biology, Medical School, Kangwon National University, Chunchon 24341, Republic of Korea. [3]Department of Pharmacology, College of Medicine, Chung-Ang University, Seoul 06974, Republic of Korea. [4]Department of Pharmacology, School of Pharmacy, Sungkyunkwan University, Suwon 16419, Republic of Korea. [5]Ginsentology Research Laboratory and Department of Physiology, College of Veterinary Medicine and Bio/Molecular Informatics Center, Konkuk University, Seoul 05029, Republic of Korea. [6]Headquarters of Forestry Support, Korea Forestry Promotion Institute, Seoul 07570, Republic of Korea. [7]Korean Society of Forest Environment Research, Namyangju 12014, Republic of Korea.

Dang *et al. Journal of Neuroinflammation* (2018) 15:52

Page 20 of 22

[8]Department of Oriental Medical Food and Nutrition, Semyung University, Jecheon 27136, Republic of Korea. [9]Department of Anatomy and Neurobiology, University of Kentucky College of Medicine, 800 Rose Street, Lexington, KY 40536, USA. [10]Neuropharmacology Section, Laboratory of Toxicology and Pharmacology, National Institute of Environmental Health Sciences, Research Triangle Park, Durham, NC 27709, USA.

References

1. Waters CM, Peck R, Rossor M, Reynolds GP, Hunt SP. Immunocytochemical studies on the basal ganglia and substantia nigra in Parkinson's disease and Huntington's chorea. Neuroscience. 1988;25:419–38.
2. Carta A, Fenu S, Morelli M. Alterations in GAD67, dynorphin and enkephalin mRNA in striatal output neurons following priming in the 6-OHDA model of Parkinson's disease. Neurol Sci. 2001;22:59–60.
3. Wang Q, Shin EJ, Nguyen XK, Li Q, Bach JH, Bing G, Kim WK, Kim HC, Hong JS. Endogenous dynorphin protects against neurotoxin-elicited nigrostriatal dopaminergic neuron damage and motor deficits in mice. J Neuroinflammation. 2012;9:124.
4. Angulo JA, McEwen BS. Molecular aspects of neuropeptide regulation and function in the corpus striatum and nucleus accumbens. Brain Res Brain Res Rev. 1994;19:1–28.
5. Martinez AN, Philipp MT. Substance P and antagonists of the neurokinin-1 receptor in neuroinflammation associated with infectious and neurodegenerative diseases of the central nervous system. J Neurol Neuromedicine. 2016;1:29–36.
6. Yu J, Cadet JL, Angulo JA. Neurokinin-1 (NK-1) receptor antagonists abrogate methamphetamine-induced striatal dopaminergic neurotoxicity in the murine brain. J Neurochem. 2002;83:613–22.
7. Yu J, Wang J, Cadet JL, Angulo JA. Histological evidence supporting a role for the striatal neurokinin-1 receptor in methamphetamine-induced neurotoxicity in the mouse brain. Brain Res. 2004;1007:124–31.
8. Gao HM, Zhou H, Hong JS. NADPH oxidases: novel therapeutic targets for neurodegenerative diseases. Trends Pharmacol Sci. 2012;33:295–303.
9. Block ML, Hong JS. Microglia and inflammation-mediated neurodegeneration: multiple triggers with a common mechanism. Prog Neurobiol. 2005;76:77–98.
10. Block ML, Zecca L, Hong JS. Microglia-mediated neurotoxicity: uncovering the molecular mechanisms. Nat Rev Neurosci. 2007;8:57–69.
11. Gao HM, Hong JS. Why neurodegenerative diseases are progressive: uncontrolled inflammation drives disease progression. Trends Immunol. 2008;29:357–65.
12. Zhang W, Shin EJ, Wang T, Lee PH, Pang H, Wie MB, Kim WK, Kim SJ, Huang WH, Wang Y, et al. 3-Hydroxymorphinan, a metabolite of dextromethorphan, protects nigrostriatal pathway against MPTP-elicited damage both in vivo and in vitro. FASEB J. 2006;20:2496–511.
13. Wang Q, Chu CH, Oyarzabal E, Jiang L, Chen SH, Wilson B, Qian L, Hong JS. Subpicomolar diphenyleneiodonium inhibits microglial NADPH oxidase with high specificity and shows great potential as a therapeutic agent for neurodegenerative diseases. Glia. 2014;62:2034–43.
14. Wang Q, Chu CH, Qian L, Chen SH, Wilson B, Oyarzabal E, Jiang L, Ali S, Robinson B, Kim HC, Hong JS. Substance P exacerbates dopaminergic neurodegeneration through neurokinin-1 receptor-independent activation of microglial NADPH oxidase. J Neurosci. 2014;34:12490–503.
15. Wang Q, Oyarzabal E, Wilson B, Qian L, Hong JS. Substance P enhances microglial density in the substantia nigra through neurokinin-1 receptor/ NADPH oxidase-mediated chemotaxis in mice. Clin Sci (Lond). 2015;129: 757–67.
16. Ritter JK, Schmidt CJ, Gibb JW, Hanson GR. Increases of substance P-like immunoreactivity within striatal-nigral structures after subacute methamphetamine treatment. J Pharmacol Exp Ther. 1984;229:487–92.
17. Ritter JK, Schmidt CJ, Gibb JW, Hanson GR. Dopamine-mediated increases in nigral substance P-like immunoreactivity. Biochem Pharmacol. 1985;34: 3161–6.
18. Hanson GR, Letter AA, Merchant K, Gibb JW. Comparison of responses by striatonigral substance P and neurokinin a systems to methamphetamine treatment. Peptides. 1986;7:983–7.
19. Chapman DE, Hanson GR, Kesner RP, Keefe KA. Long-term changes in basal ganglia function after a neurotoxic regimen of methamphetamine. J Pharmacol Exp Ther. 2001;296:520–7.
20. Hong JS, Yang HT, Costa E. Substance P content of substantia nigra after chronic treatment with antischizophrenic drugs. Neuropharmacology. 1978; 17:83–5.
21. Hanson G, Alphs L, Pradhan S, Lovenberg W. Response of striatonigral substance P systems to a dopamine receptor agonist and antagonist. Neuropharmacology. 1981;20:541–8.
22. Hanson GR, Alphs L, Wolf W, Levine R, Lovenberg W. Haloperidol-induced reduction of nigral substance P-like immunoreactivity: a probe for the interactions between dopamine and substance P neuronal systems. J Pharmacol Exp Ther. 1981;218:568–74.
23. Block ML, Li G, Qin L, Wu X, Pei Z, Wang T, Wilson B, Yang J, Hong JS. Potent regulation of microglia-derived oxidative stress and dopaminergic neuron survival: substance P vs. dynorphin. FASEB J. 2006;20:251–8.
24. Xie JT, Shao ZH, Vanden Hoek TL, Chang WT, Li J, Mehendale S, Wang CZ, Hsu CW, Becker LB, Yin JJ, Yuan CS. Antioxidant effects of ginsenoside Re in cardiomyocytes. Eur J Pharmacol. 2006;532:201–7.
25. Bai CX, Sunami A, Namiki T, Sawanobori T, Furukawa T. Electrophysiological effects of ginseng and ginsenoside Re in guinea pig ventricular myocytes. Eur J Pharmacol. 2003;476:35–44.
26. Bai CX, Takahashi K, Masumiya H, Sawanobori T, Furukawa T. Nitric oxide-dependent modulation of the delayed rectifier K+ current and the L-type Ca^{2+} current by ginsenoside Re, an ingredient of Panax ginseng, in guinea-pig cardiomyocytes. Br J Pharmacol. 2004;142:567–75.
27. Kim HS, Lee JH, Goo YS, Nah SY. Effects of ginsenosides on Ca^{2+} channels and membrane capacitance in rat adrenal chromaffin cells. Brain Res Bull. 1998;46:245–51.
28. Kim KH, Song K, Yoon SH, Shehzad O, Kim YS, Son JH. Rescue of PINK1 protein null-specific mitochondrial complex IV deficits by ginsenoside Re activation of nitric oxide signaling. J Biol Chem. 2012;287:44109–20.
29. Xu BB, Liu CQ, Gao X, Zhang WQ, Wang SW, Cao YL. Possible mechanisms of the protection of ginsenoside Re against MPTP-induced apoptosis in substantia nigra neurons of Parkinson's disease mouse model. J Asian Nat Prod Res. 2005;7:215–24.
30. Shin EJ, Shin SW, Nguyen TT, Park DH, Wie MB, Jang CG, Nah SY, Yang BW, Ko SK, Nabeshima T, Kim HC. Ginsenoside Re rescues methamphetamine-induced oxidative damage, mitochondrial dysfunction, microglial activation, and dopaminergic degeneration by inhibiting the protein kinase Cdelta gene. Mol Neurobiol. 2014;49:1400–21.
31. Dang DK TH, Shin EJ, Jang CG, Jeong JH, Byun JK, Ko SK, Kim HC: Ginsenoside Re protects methamphetamine neurotoxicity via up-regulation of dynorphin-mediated κ-receptor and down-regulation of neurokinin 1 receptor in mice (abstract).. Proceedings of the spring international convention of the pharmaceutical society of Korea, Seoul, April 20–21 The Pharmaceutical Society of Korea 2017:364.
32. Sharifi N, Diehl N, Yaswen L, Brennan MB, Hochgeschwender U. Generation of dynorphin knockout mice. Brain Res Mol Brain Res. 2001;86:70–5.
33. Nguyen XV, Liu M, Kim HC, Bing G. Effects of prodynorphin deletion on striatal dopamine in mice during normal aging and in response to MPTP. Exp Neurol. 2009;219:228–38.
34. Shin EJ, Jang CG, Bing G, Park DH, Oh CH, Koo KH, Oh KW, Yamada K, Nabeshima T, Kim HC. Prodynorphin gene deficiency potentiates nalbuphine-induced behavioral sensitization and withdrawal syndrome in mice. Drug Alcohol Depend. 2009;104:175–84.
35. Ko SK, Bae HM, Cho OS, BO IM, Chung SH, Lee BY. Analysis of ginsenoside composition of ginseng berry and seed. Food Sci Biotechnol. 2008;17:1379–82.
36. Ko SK, Cho OS, Bae HM, Im BO, Lee OH, Lee BY. Quantitative analysis of ginsenosides composition in flower buds of various ginseng plants. J Korean Soc Appl Biol Chem. 2011;54:154–7.
37. Shigematsu N, Fukuda T, Yamamoto T, Nishioku T, Yamaguchi T, Himeno M, Nakayama KI, Tsukuba T, Kadowaki T, Okamoto K, et al. Association of cathepsin E deficiency with the increased territorial aggressive response of mice. J Neurochem. 2008;105:1394–404.
38. Al-Hasani R, McCall JG, Shin G, Gomez AM, Schmitz GP, Bernardi JM, Pyo CO, Park SI, Marcinkiewcz CM, Crowley NA, et al. Distinct subpopulations of nucleus accumbens dynorphin neurons drive aversion and reward. Neuron. 2015;87:1063–77.
39. Shin EJ, Duong CX, Nguyen XT, Li Z, Bing G, Bach JH, Park DH, Nakayama K, Ali SF, Kanthasamy AG, et al. Role of oxidative stress in methamphetamine-induced dopaminergic toxicity mediated by protein kinase Cdelta. Behav Brain Res. 2012;232:98–113.

Dang *et al. Journal of Neuroinflammation* (2018) 15:52

Page 21 of 22

40. Maximova OA, Taffs RE, Pomeroy KL, Piccardo P, Asher DM. Computerized morphometric analysis of pathological prion protein deposition in scrapie-infected hamster brain. J Histochem Cytochem. 2006;54:97–107.

41. Pellegrino D, Cicchetti F, Wang X, Zhu A, Yu M, Saint-Pierre M, Brownell AL. Modulation of dopaminergic and glutamatergic brain function: PET studies on parkinsonian rats. J Nucl Med. 2007;48:1147–53.

42. Castano A, Cano J, Machado A. Low selenium diet affects monoamine turnover differentially in substantia nigra and striatum. J Neurochem. 1993;61:1302–7.

43. Kim HC, Jhoo WK, Choi DY, Im DH, Shin EJ, Suh JH, Floyd RA, Bing G. Protection of methamphetamine nigrostriatal toxicity by dietary selenium. Brain Res. 1999;851:76–86.

44. Kim WG, Mohney RP, Wilson B, Jeohn GH, Liu B, Hong JS. Regional difference in susceptibility to lipopolysaccharide-induced neurotoxicity in the rat brain: role of microglia. J Neurosci. 2000;20:6309–16.

45. Tran HY, Shin EJ, Saito K, Nguyen XK, Chung YH, Jeong JH, Bach JH, Park DH, Yamada K, Nabeshima T, et al. Protective potential of IL-6 against trimethyltin-induced neurotoxicity in vivo. Free Radic Biol Med. 2012;52:1159–74.

46. Nguyen XK, Lee J, Shin EJ, Dang DK, Jeong JH, Nguyen TT, Nam Y, Cho HJ, Lee JC, Park DH, et al. Liposomal melatonin rescues methamphetamine-elicited mitochondrial burdens, pro-apoptosis, and dopaminergic degeneration through the inhibition PKCdelta gene. J Pineal Res. 2015;58:86–106.

47. Oliver CN, Ahn BW, Moerman EJ, Goldstein S, Stadtman ER. Age-related changes in oxidized proteins. J Biol Chem. 1987;262:5488–91.

48. Shin EJ, Nam Y, Lee JW, Nguyen PT, Yoo JE, Tran TV, Jeong JH, Jang CG, Oh YJ, Youdim MBH, et al. N-methyl, N-propynyl-2-phenylethylamine (MPPE), a selegiline analog, attenuates MPTP-induced dopaminergic toxicity with guaranteed behavioral safety: involvement of inhibitions of mitochondrial oxidative burdens and p53 gene-elicited pro-apoptotic change. Mol Neurobiol. 2016;53:6251–69.

49. Holzer P, Schluet W, Maggi CA. Substance P stimulates and inhibits intestinal peristalsis via distinct receptors. J Pharmacol Exp Ther. 1995;274:322–8.

50. Jayanthi S, Deng X, Bordelon M, McCoy MT, Cadet JL. Methamphetamine causes differential regulation of pro-death and anti-death Bcl-2 genes in the mouse neocortex. FASEB J. 2001;15:1745–52.

51. Imam SZ, Itzhak Y, Cadet JL, Islam F, Slikker W Jr, Ali SF. Methamphetamine-induced alteration in striatal p53 and bcl-2 expressions in mice. Brain Res Mol Brain Res. 2001;91:174–8.

52. Cadet JL, Jayanthi S, Deng X. Methamphetamine-induced neuronal apoptosis involves the activation of multiple death pathways. Review. Neurotox Res. 2005;8:199–206.

53. Zhu JP, Xu W, Angulo N, Angulo JA. Methamphetamine-induced striatal apoptosis in the mouse brain: comparison of a binge to an acute bolus drug administration. Neurotoxicology. 2006;27:131–6.

54. Zhu J, Xu W, Wang J, Ali SF, Angulo JA. The neurokinin-1 receptor modulates the methamphetamine-induced striatal apoptosis and nitric oxide formation in mice. J Neurochem. 2009;111:656–68.

55. Dang DK, Shin EJ, Nam Y, Ryoo S, Jeong JH, Jang CG, Nabeshima T, Hong JS, Kim HC. Apocynin prevents mitochondrial burdens, microglial activation, and pro-apoptosis induced by a toxic dose of methamphetamine in the striatum of mice via inhibition of p47phox activation by ERK. J Neuroinflammation. 2016;13:12.

56. Dang DK, Shin EJ, Kim DJ, Tran HQ, Jeong JH, Jang CG, Ottersen OP, Nah SY, Hong JS, Nabeshima T, Kim HC. PKCdelta-dependent p47phox activation mediates methamphetamine-induced dopaminergic neurotoxicity. Free Radic Biol Med. 2017;115:318–37.

57. Shin EJ, Tran HQ, Nguyen PT, Jeong JH, Nah SY, Jang CG, Nabeshima T, Kim HC. Role of mitochondria in methamphetamine-induced dopaminergic neurotoxicity: involvement in oxidative stress, neuroinflammation, and pro-apoptosis-a review. Neurochem Res. 2017;43(1):57–69.

58. Nam Y, Wie MB, Shin EJ, Nguyen TT, Nah SY, Ko SK, Jeong JH, Jang CG, Kim HC. Ginsenoside Re protects methamphetamine-induced mitochondrial burdens and proapoptosis via genetic inhibition of protein kinase C delta in human neuroblastoma dopaminergic SH-SY5Y cell lines. J Appl Toxicol. 2015;35:927–44.

59. Tulloch I, Afanador L, Mexhitaj I, Ghazaryan N, Garzagongora AG, Angulo JA. A single high dose of methamphetamine induces apoptotic and necrotic striatal cell loss lasting up to 3 months in mice. Neuroscience. 2011;193:162–9.

60. Dang DK, Shin EJ, Tran HQ, Kim DJ, Jeong JH, Jang CG, Nah SY, Sato H, Nabeshima T, Yoneda Y, Kim HC. The role of system xc (–) in methamphetamine-induced dopaminergic neurotoxicity in mice. Neurochem Int. 2017;108:254–65.

61. Wilson JM, Levey AI, Rajput A, Ang L, Guttman M, Shannak K, Niznik HB, Hornykiewicz O, Pifl C, Kish SJ. Differential changes in neurochemical markers of striatal dopamine nerve terminals in idiopathic Parkinson's disease. Neurology. 1996;47:718–26.

62. Wilson JM, Kalasinsky KS, Levey AI, Bergeron C, Reiber G, Anthony RM, Schmunk GA, Shannak K, Haycock JW, Kish SJ. Striatal dopamine nerve terminal markers in human, chronic methamphetamine users. Nat Med. 1996;2:699–703.

63. Seiden LS, Sabol KE. Methamphetamine and methylenedioxymethamphetamine neurotoxicity: possible mechanisms of cell destruction. NIDA Res Monogr. 1996;163:251–76.

64. El Daly E, Chefer V, Sandill S, Shippenberg TS. Modulation of the neurotoxic effects of methamphetamine by the selective kappa-opioid receptor agonist U69593. J Neurochem. 2000;74:1553–62.

65. Chefer VI, Moron JA, Hope B, Rea W, Shippenberg TS. Kappa-opioid receptor activation prevents alterations in mesocortical dopamine neurotransmission that occur during abstinence from cocaine. Neuroscience. 2000;101:619–27.

66. Heidbreder CA, Goldberg SR, Shippenberg TS. The kappa-opioid receptor agonist U-69593 attenuates cocaine-induced behavioral sensitization in the rat. Brain Res. 1993;616:335–8.

67. Heidbreder CA, Babovic-Vuksanovic D, Shoaib M, Shippenberg TS. Development of behavioral sensitization to cocaine: influence of kappa opioid receptor agonists. J Pharmacol Exp Ther. 1995;275:150–63.

68. Shippenberg TS, Elmer GI. The neurobiology of opiate reinforcement. Crit Rev Neurobiol. 1998;12:267–303.

69. You ZB, Herrera-Marschitz M, Terenius L. Modulation of neurotransmitter release in the basal ganglia of the rat brain by dynorphin peptides. J Pharmacol Exp Ther. 1999;290:1307–15.

70. Schoffelmeer AN, Hogenboom F, Mulder AH. Kappa1- and kappa2-opioid receptors mediating presynaptic inhibition of dopamine and acetylcholine release in rat neostriatum. Br J Pharmacol. 1997;122:520–4.

71. Shippenberg TS, Chefer VI, Zapata A, Heidbreder CA. Modulation of the behavioral and neurochemical effects of psychostimulants by kappa-opioid receptor systems. Ann N Y Acad Sci. 2001;937:50–73.

72. Zeynalov E, Nemoto M, Hurn PD, Koehler RC, Bhardwaj A. Neuroprotective effect of selective kappa opioid receptor agonist is gender specific and linked to reduced neuronal nitric oxide. J Cereb Blood Flow Metab. 2006;26:414–20.

73. Toyoshi T, Ukai M, Kameyama T. Opioid receptor agonists selective for mu and kappa receptors attenuate methamphetamine-induced behavioral sensitization in the mouse. Biol Pharm Bull. 1996;19:369–74.

74. Mari M, Morales A, Colell A, Garcia-Ruiz C, Kaplowitz N, Fernandez-Checa JC. Mitochondrial glutathione: features, regulation and role in disease. Biochim Biophys Acta. 2013;830:3317–28.

75. Coyle JT, Puttfarcken P. Oxidative stress, glutamate, and neurodegenerative disorders. Science. 1993;262:689–95.

76. Halliwell B. Reactive oxygen species and the central nervous system. J Neurochem. 1992;59:1609–23.

77. Hirata H, Ladenheim B, Rothman RB, Epstein C, Cadet JL. Methamphetamine-induced serotonin neurotoxicity is mediated by superoxide radicals. Brain Res. 1995;677:345–7.

78. Soltoff SP, Toker A. Carbachol, substance P, and phorbol ester promote the tyrosine phosphorylation of protein kinase C delta in salivary gland epithelial cells. J Biol Chem. 1995;270:13490–5.

79. Koon HW, Zhao D, Zhan Y, Simeonidis S, Moyer MP, Pothoulakis C. Substance P-stimulated interleukin-8 expression in human colonic epithelial cells involves protein kinase Cdelta activation. J Pharmacol Exp Ther. 2005;314:1393–400.

80. Ramnath RD, Sun J, Adhikari S, Zhi L, Bhatia M. Role of PKC-delta on substance P-induced chemokine synthesis in pancreatic acinar cells. Am J Physiol Cell Physiol. 2008;294:C683–92.

81. Sonsalla PK, Gibb JW, Hanson GR. Nigrostriatal dopamine actions on the D2 receptors mediate methamphetamine effects on the striatonigral substance P system. Neuropharmacology. 1986;25:1221–30.

82. Bannon MJ, Elliott PJ, Bunney EB. Striatal tachykinin biosynthesis: regulation of mRNA and peptide levels by dopamine agonists and antagonists. Brain Res. 1987;427:31–7.

Dang *et al. Journal of Neuroinflammation* (2018) 15:52

Page 22 of 22

83. Zhang Y, Landas K, Mueller H, Angulo JA. Progressive augmentation of striatal and accumbal preprotachykinin mRNA levels by chronic treatment with methamphetamine and effect of concurrent administration of the N-methyl-D-aspartate receptor antagonist MK-801. Neuropharmacology. 1997;36:325–34.

84. Mantyh PW, Johnson DJ, Boehmer CG, Catton MD, Vinters HV, Maggio JE, Too HP, Vigna SR. Substance P receptor binding sites are expressed by glia in vivo after neuronal injury. Proc Natl Acad Sci U S A. 1989;86:5193–7.

85. Marriott I. The role of tachykinins in central nervous system inflammatory responses. Front Biosci. 2004;9:2153–65.

86. Anderson KD, Reiner A. Extensive co-occurrence of substance P and dynorphin in striatal projection neurons: an evolutionarily conserved feature of basal ganglia organization. J Comp Neurol. 1990;295:339–69.

87. Hastings TG, Lewis DA, Zigmond MJ. Reactive dopamine metabolites and neurotoxicity: implications for Parkinson's disease. Adv Exp Med Biol. 1996; 387:97–106.

88. Hastings TG, Zigmond MJ. Loss of dopaminergic neurons in parkinsonism: possible role of reactive dopamine metabolites. J Neural Transm Suppl. 1997;49:103–10.

89. Mosley RL, Benner EJ, Kadiu I, Thomas M, Boska MD, Hasan K, Laurie C, Gendelman HE. Neuroinflammation, oxidative stress and the pathogenesis of Parkinson's disease. Clin Neurosci Res. 2006;6:261–81.

90. Reynolds A, Laurie C, Mosley RL, Gendelman HE. Oxidative stress and the pathogenesis of neurodegenerative disorders. Int Rev Neurobiol. 2007;82: 297–325.

91. Kim HC, Jhoo WK, Shin EJ, Bing G. Selenium deficiency potentiates methamphetamine-induced nigral neuronal loss; comparison with MPTP model. Brain Res. 2000;862:247–52.

92. Brownstein MJ, Mroz EA, Tappaz ML, Leeman SE. On the origin of substance P and glutamic acid decarboxylase (GAD) in the substantia nigra. Brain Res. 1977;135:315–23.

93. Hong JS, Yang HY, Racagni G, Costa E. Projections of substance P containing neurons from neostriatum to substantia nigra. Brain Res. 1977; 122:541–4.

94. Marksteiner J, Saria A, Krause JE. Comparative distribution of neurokinin B-, substance P- and enkephalin-like immunoreactivities and neurokinin B messenger RNA in the basal forebrain of the rat: evidence for neurochemical compartmentation. Neuroscience. 1992;51:107–20.

95. Dray A. The physiology and pharmacology of mammalian basal ganglia. Prog Neurobiol. 1980;14:221–335.

96. Walker RJ, Kemp JA, Yajima H, Kitagawa K, Woodruff GN. The action of substance P on mesencephalic reticular and substantia nigral neurones of the rat. Experientia. 1976;32:214–5.

97. Qin L, Wu X, Block ML, Liu Y, Breese GR, Hong JS, Knapp DJ, Crews FT. Systemic LPS causes chronic neuroinflammation and progressive neurodegeneration. Glia. 2007;55:453–62.

98. Liu B, Qin L, Yang SN, Wilson BC, Liu Y, Hong JS. Femtomolar concentrations of dynorphins protect rat mesencephalic dopaminergic neurons against inflammatory damage. J Pharmacol Exp Ther. 2001;298: 1133–41.

99. Krasnova IN, Cadet JL. Methamphetamine toxicity and messengers of death. Brain Res Rev. 2009;60:379–407.

100. Kong LY, McMillian MK, Hudson PM, Jin L, Hong JS. Inhibition of lipopolysaccharide-induced nitric oxide and cytokine production by ultralow concentrations of dynorphins in mixed glia cultures. J Pharmacol Exp Ther. 1997;280:61–6.

101. Eisch AJ, Gaffney M, Weihmuller FB, O'Dell SJ, Marshall JF. Striatal subregions are differentially vulnerable to the neurotoxic effects of methamphetamine. Brain Res. 1992;598:321–6.

102. Fumagalli F, Gainetdinov RR, Valenzano KJ, Caron MG. Role of dopamine transporter in methamphetamine-induced neurotoxicity: evidence from mice lacking the transporter. J Neurosci. 1998;18:4861–9.

103. Abekawa T, Ohmori T, Koyama T. Effects of repeated administration of a high dose of methamphetamine on dopamine and glutamate release in rat striatum and nucleus accumbens. Brain Res. 1994;643:276–81.

104. Hurd YL, Herkenham M. Influence of a single injection of cocaine, amphetamine or GBR 12909 on mRNA expression of striatal neuropeptides. Brain Res Mol Brain Res. 1992;16:97–104.

105. Wang JQ, McGinty JF. D1 and D2 receptor regulation of preproenkephalin and preprodynorphin mRNA in rat striatum following acute injection of amphetamine or methamphetamine. Synapse. 1996;22:114–22.

106. Harvey DC, Lacan G, Melegan WP. Regional heterogeneity of dopaminergic deficits in vervet monkey striatum and substantia nigra after methamphetamine exposure. Exp Brain Res. 2000;133:349–58.

107. Harvey DC, Lacan G, Tanious SP, Melega WP. Recovery from methamphetamine induced long-term nigrostriatal dopaminergic deficits without substantia nigra cell loss. Brain Res. 2000;871:259–70.

108. Joo KM, Lee JH, Jeon HY, Park CW, Hong DK, Jeong HJ, Lee SJ, Lee SY, Lim KM. Pharmacokinetic study of ginsenoside Re with pure ginsenoside Re and ginseng berry extracts in mouse using ultra performance liquid chromatography/mass spectrometric method. J Pharm Biomed Anal. 2010; 51:278–83.

109. Kim YK, Yoo DS, Xu H, Park NI, Kim HH, Choi JE, Park SU. Ginsenoside content of berries and roots of three typical Korean ginseng (Panax ginseng) cultivars. Nat Prod Commun. 2009;4:903–6.